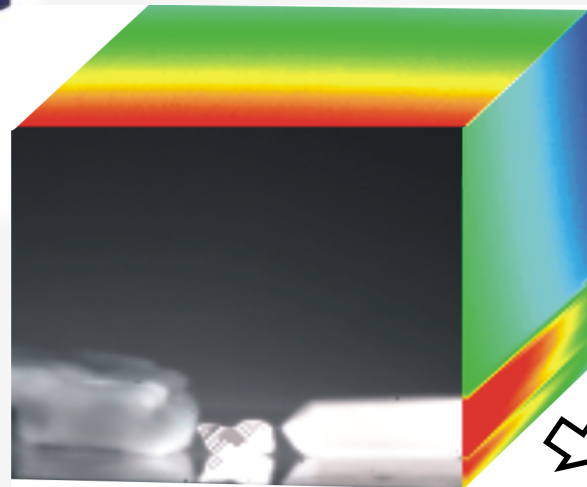
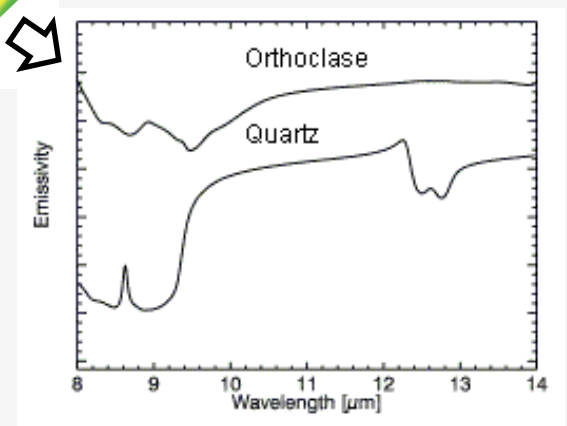




Uncertainties in TIR Hyperspectral Image Cube Unmixing



Keshav D Singh (Postdoc)
UC Davis, CA





Research Objective

“To study and model the influencing factors that contributes non-linear spectral mixing in the Thermal Infrared (TIR) region”



Spectral Mixing Models

Linear Mixing Model (LMM):

[Keshava et al., 2002, 2003]

- It assumes no interaction between materials
- The mixed spectrum is a linear combination of ground cover radiance spectra

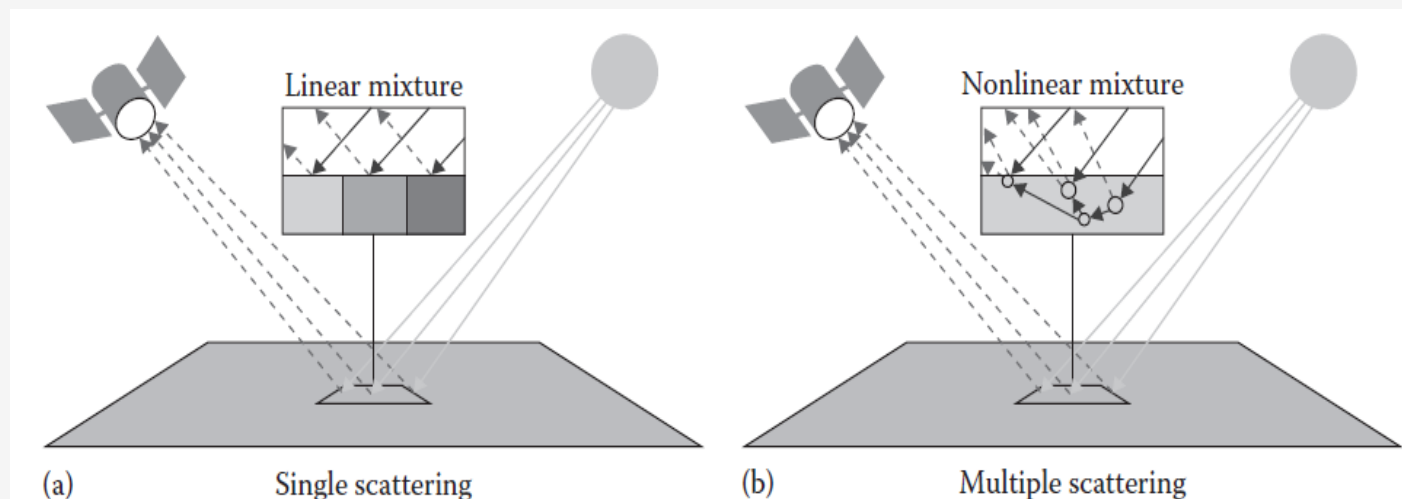
$$b(\lambda) = \sum_{i=1}^q a_i(\lambda)x_i + \text{err}(\lambda) = \mathbf{A}\mathbf{x} + \eta(\lambda); \quad \text{OR} \quad \mathbf{r}_i = \sum_{i=1}^q m_i \xi_i + \eta_i = \mathbf{M}\xi + \eta$$

Non-linear Mixing Model (NLMM):

[Hapke, 1981; Bioucas Dias et al., 2007]

- It assumes multiple scattering due to intimate mixture (particulate media)
- Using model-based unmixing one can only know the functional formulation of \mathbf{f} as,

$$\mathbf{r}_i = \mathbf{f}(\{m_i\}_i, \{x_i\}_i, \rho, \eta; \lambda)$$





Why LMM to NLMM?

- Scale of mixing is large, or macroscopic: Linear Mixture
Microscopic or intimate mixtures: Non-linear Mixture
- Linear model is only valid where the endmembers are arranged in discrete patches on the surface, as there is no significant occurrence of multiple scattering between the different surface components. *This condition is almost never met in nature.*
- The medium cannot be considered as a continuous medium, interference occurs between the portions of light scattered by the particles.
- Shadowing of one particle by another particle occurs, as a result of which a particle is not able to scatter or absorb light to its full potential.

The overwhelming uncertainties are associated with endmember extraction using LMM, that's why for non-linear spectral unmixing a radiative transfer based model need to be develop.

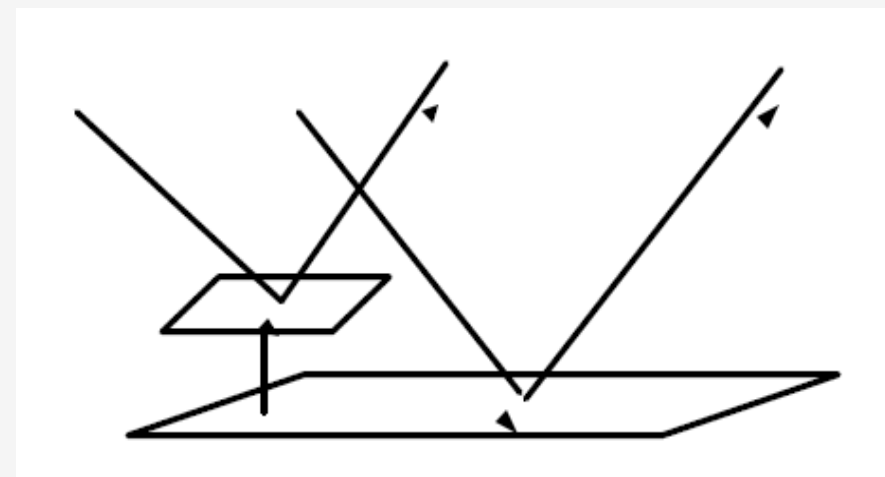


Non-linearity in TIR Domain

What THRS community Believes

- Spectral mixing phenomenon in emissive (TIR) domain is purely a linear process

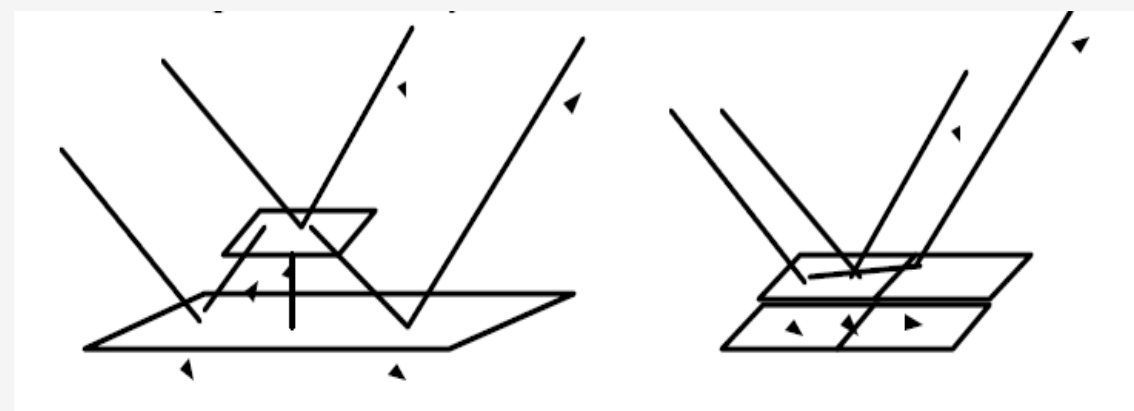
[Moersch and Christensen, 1995; Ramsey and Christensen 1998; Van der Meer et al., 2006; Nowicki and Christensen 2007; Rogers and Christensen 2007]



What NIR-SWIR community Realized

- Grain size and Fabric variations on emissivity spectra
- Parameters influencing non-linearity in emissivity spectra

[Fontanilles and Briottet, 2011; Danilia et al., 2012, Singh and Ramakrishnan, 2015]

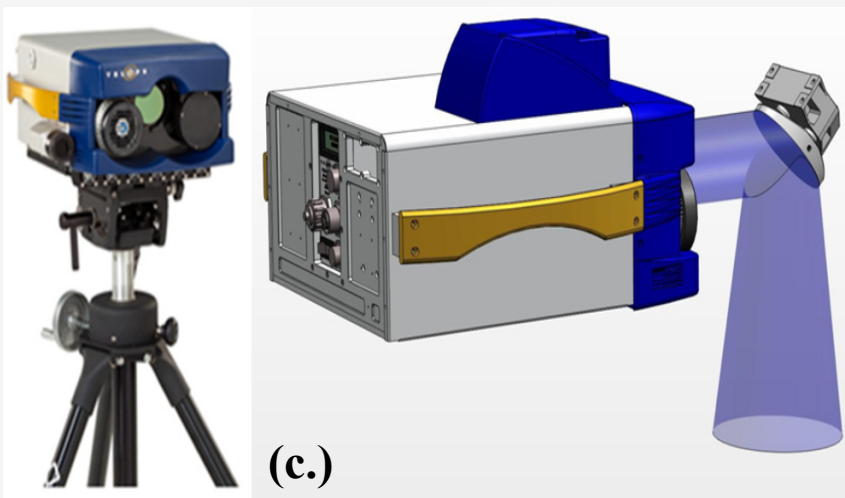
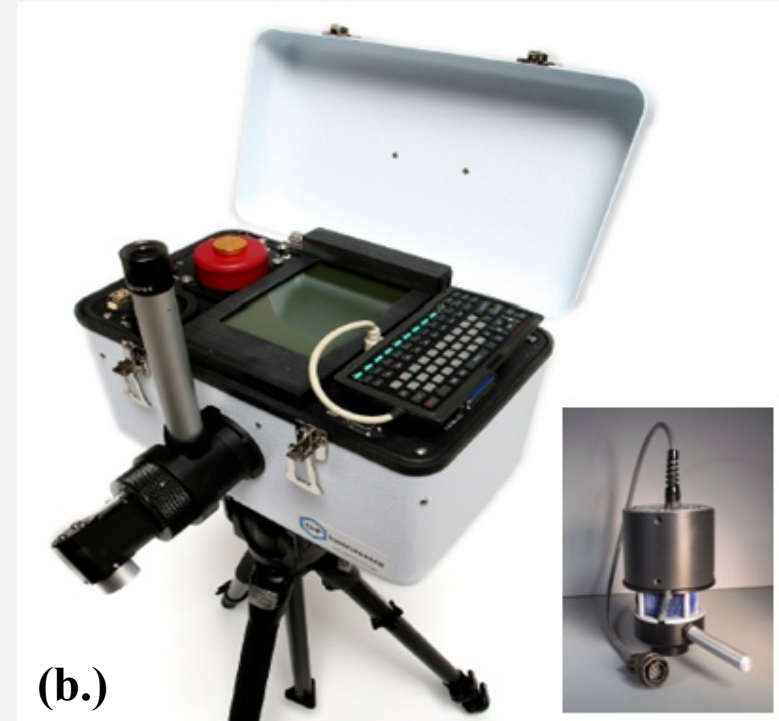
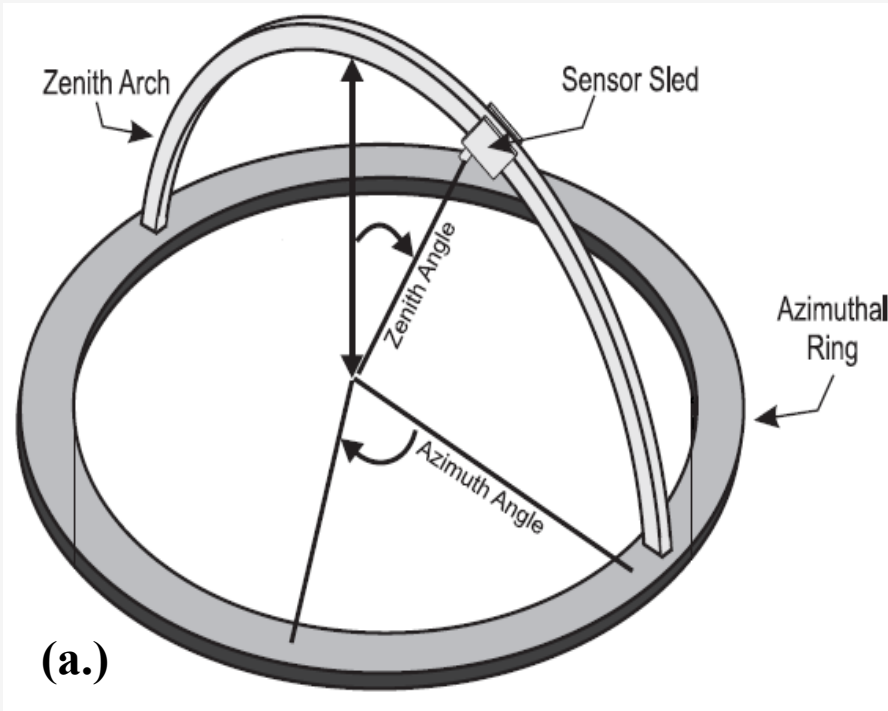


Non-linear Vertical Mixing, e.g. Light in tree canopies

Non-linear Horizontal Mixing, e.g. Granular mixtures



Experimental Instruments



(a.) Source-sensor geometry in a Goniometer system.

(c.) Fourier Transform Infrared Spectrometer (FTIR[®]) @2-16 μm with Black Body (NIR to TIR Region).

(b.) Hyper-Cam-LW Imager @8-12 μm (TIR Region).



Experimental Setup

Data Acquisition: FTIR spectrometer (2-16 μ m)

Fore optics FOV: 4.8°

Sample pattern diameter: 3-inchs

Experimental Sample Sets:

- (i) **Two component mineral system:** quartz, orthoclase feldspar, and amphibole of grain size (2–4mm, 0.7–2 mm, 0.5–0.063 mm and <0.063 mm)
- (ii) **Two component rock system:** anorthosite and quartzite of grain size (2.36–4mm, 1–2.36mm and $\leq 75\mu$ m)
- (iii) **Three component rock system:** anorthosite, quartzite and basalt of grain size (2.36–4mm, 1–2.36mm and $\leq 75\mu$ m)



Experimental Steps

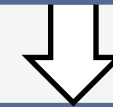
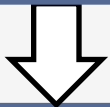
I. Sample Preparation

- Samples : Basalt (B), Anorthosite (A), Quartzite (Q)
- Grain size/ texture ranges: 2-4mm, 1-2mm, <1mm
- Seven patterns/ fabrics were studied.



II. Data Acquisition

- D&P-102 FTIR (2–16 μm)
- Sensor height=45.00cm; IFOV=25°; Radius of FOV~9.976cm
- $i=5^\circ$, $\psi = 0-180^\circ @ 30^\circ$ increment, $e = -20^\circ$ to $+20^\circ @ 5^\circ$ increment



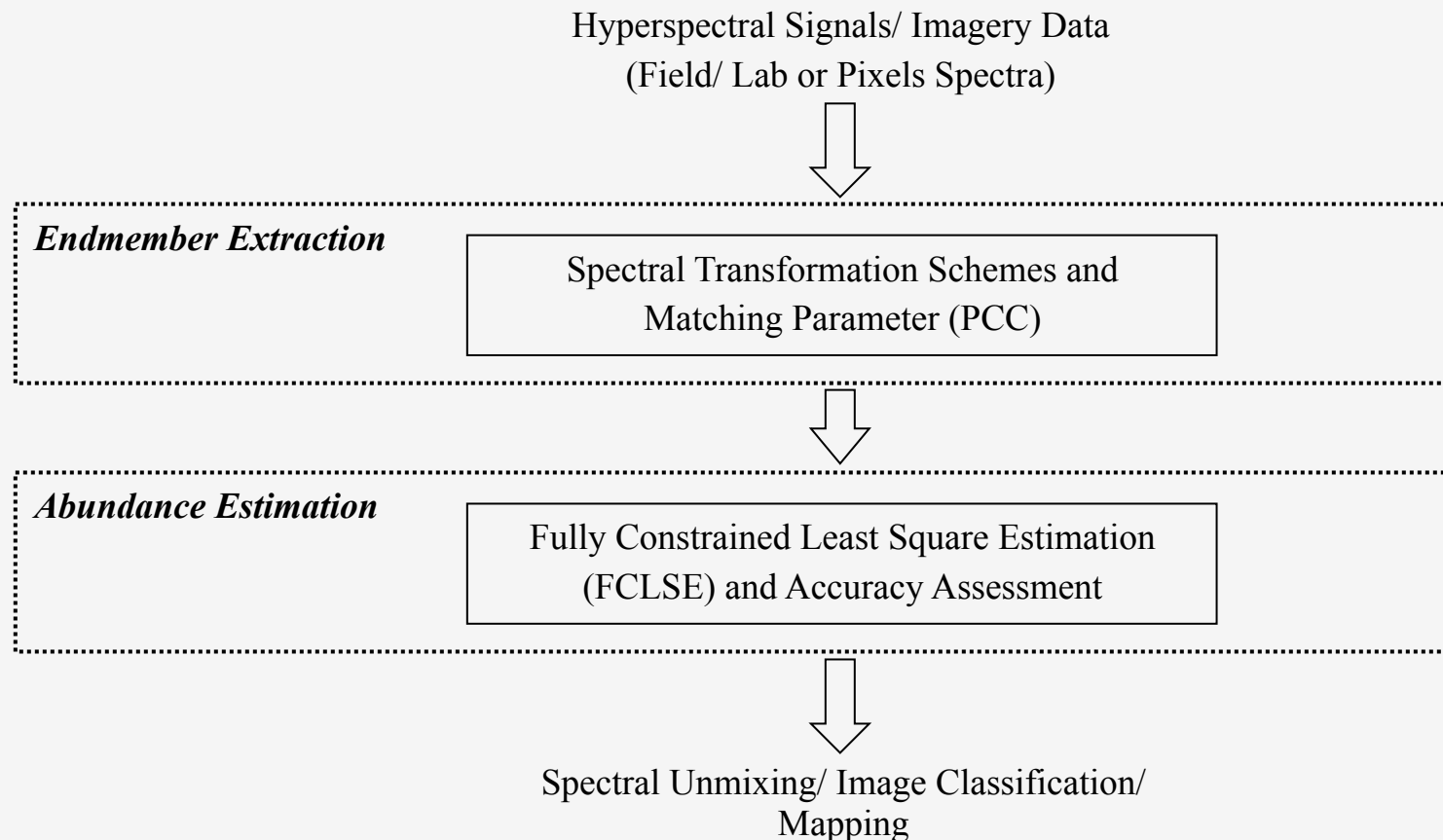
III. Data Processing and Interpretation

- Model parameter for 54- geometry, 7- patterns and 3- grain sizes were obtained by minimizing RMSE
- Analysis for scattering anisotropy and spectral shape/depth changes



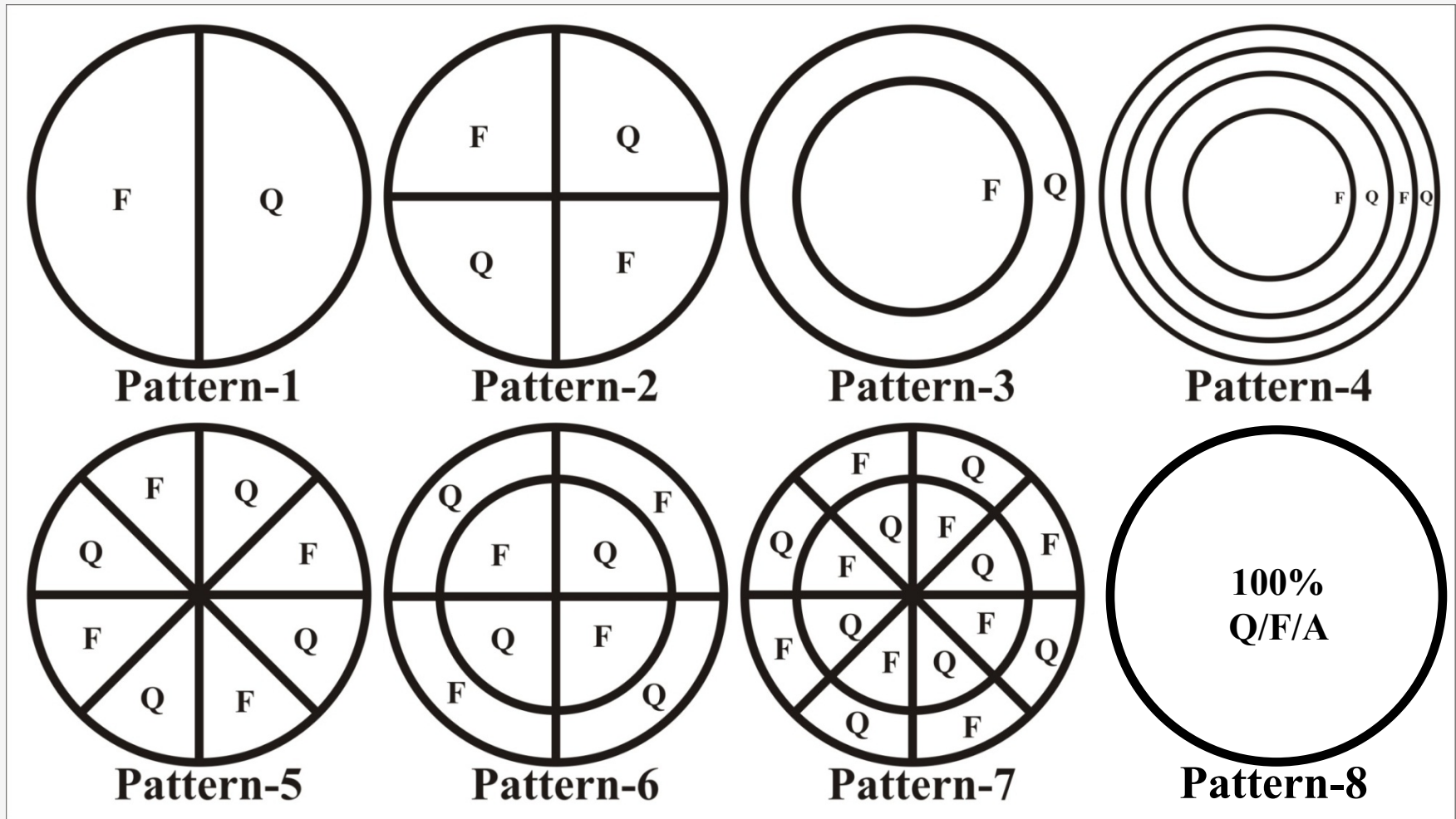
Methodology Used

The basic methodological steps used from Hyperspectral signal to *feature extraction* and *abundance estimation*



Two Component Mineral System (Q-A; Q-F)

Two Component System (Quartz-Feldspar/Amphibole)



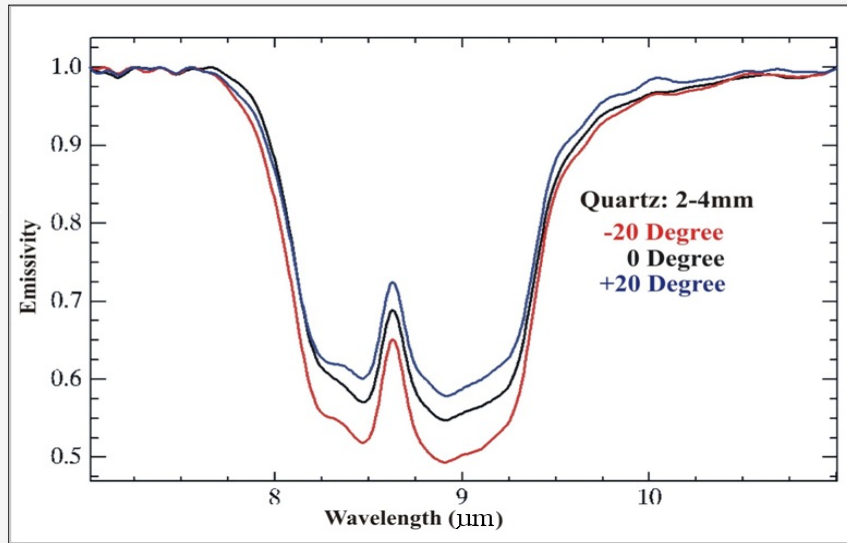
8 patterns × 4 grain sizes



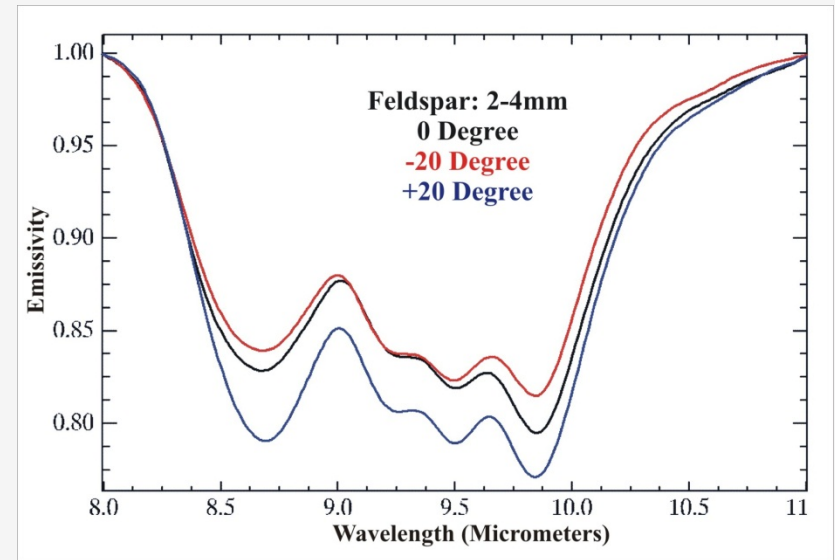
Effect of Geometry on IR-spectra (Q, F, A)



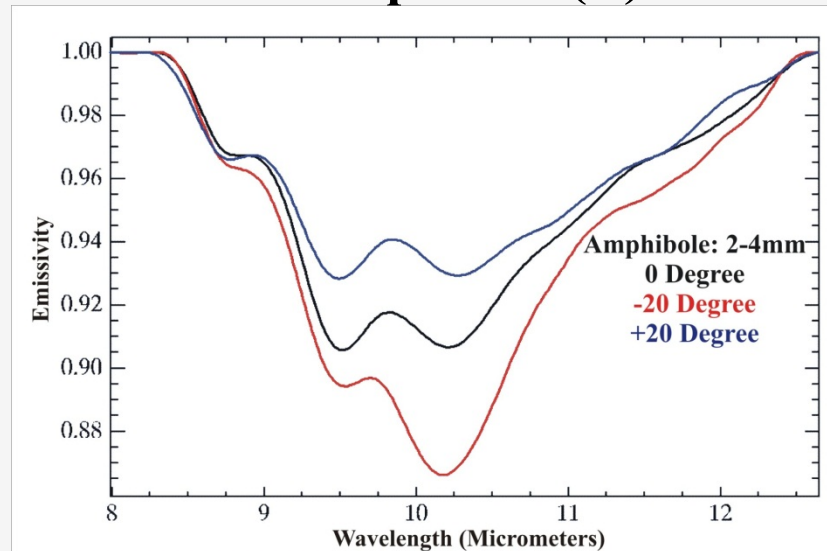
Quartz (Q)



Feldspar (F)



Amphibole (A)



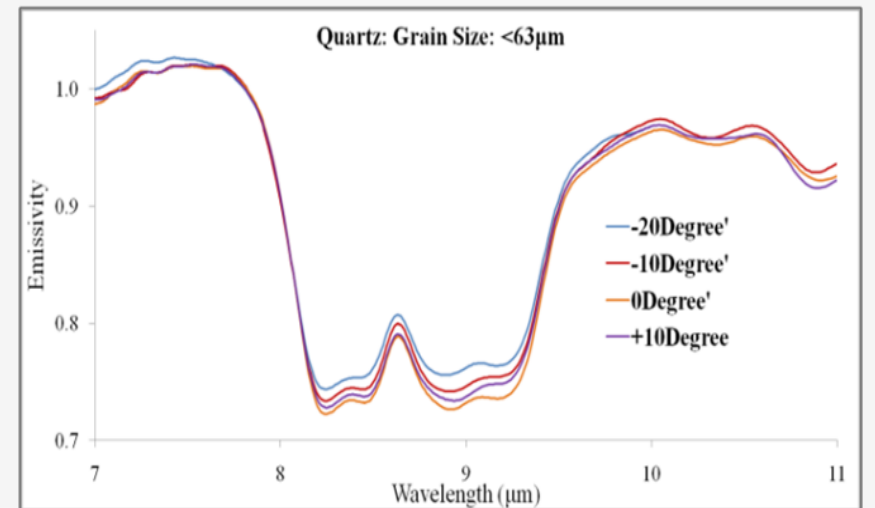
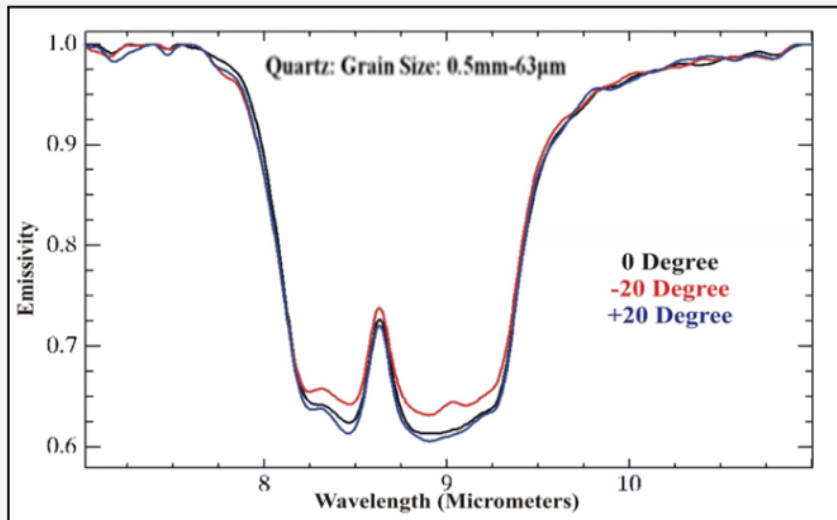
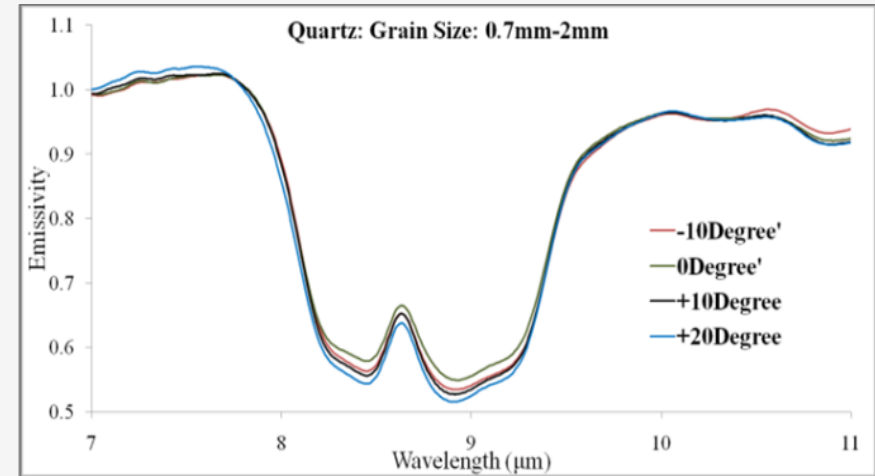
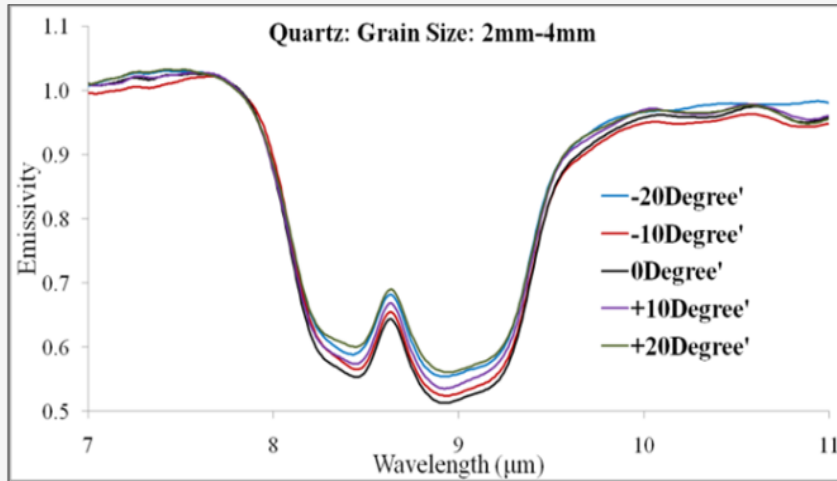
Variation in absorption feature



Effect of Grain Size on IR-spectra (Quartz)

Variation with grain size

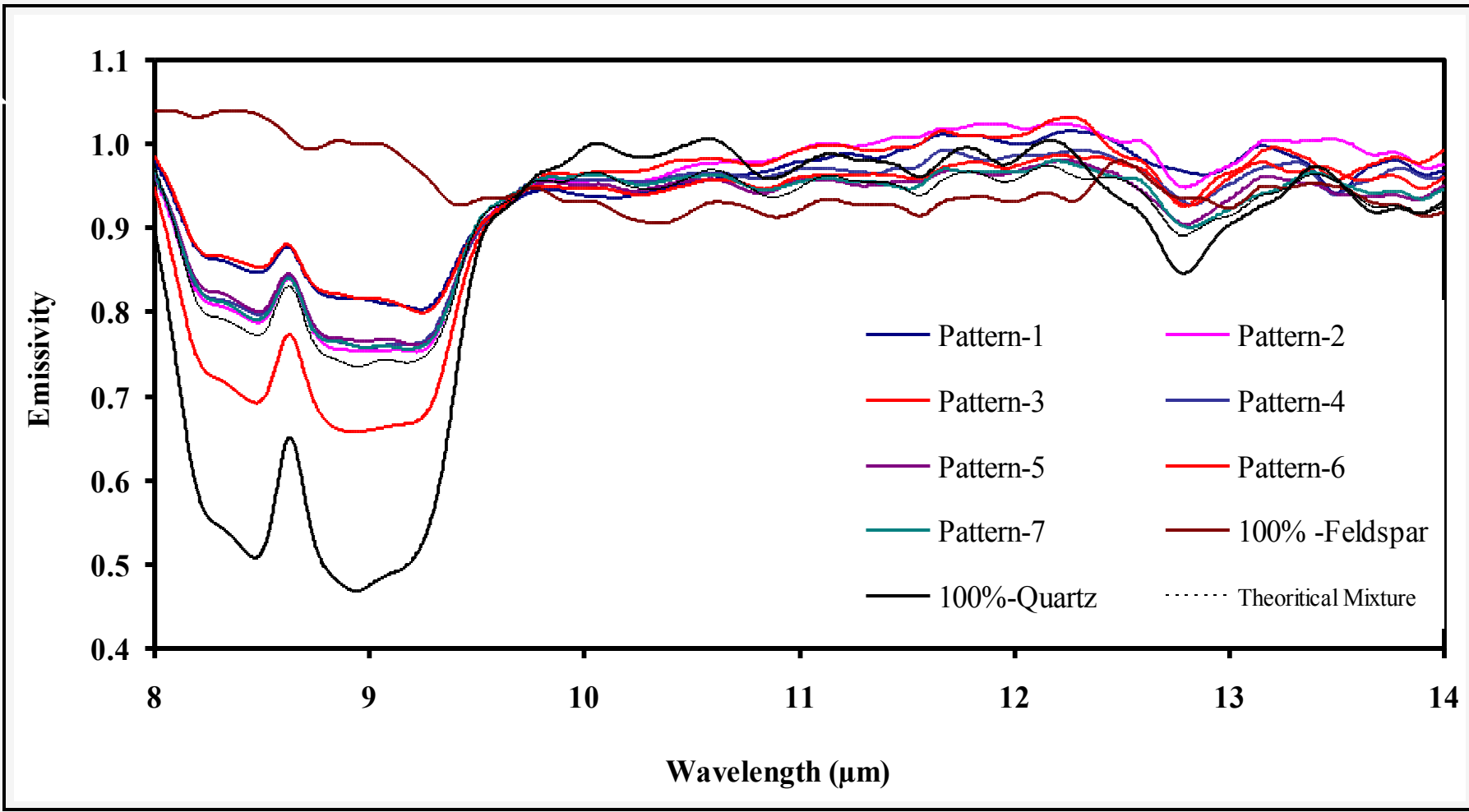
Variation in absorption feature





Effect of Fabric on IR-spectra (Q-A)

Variation in absorption feature

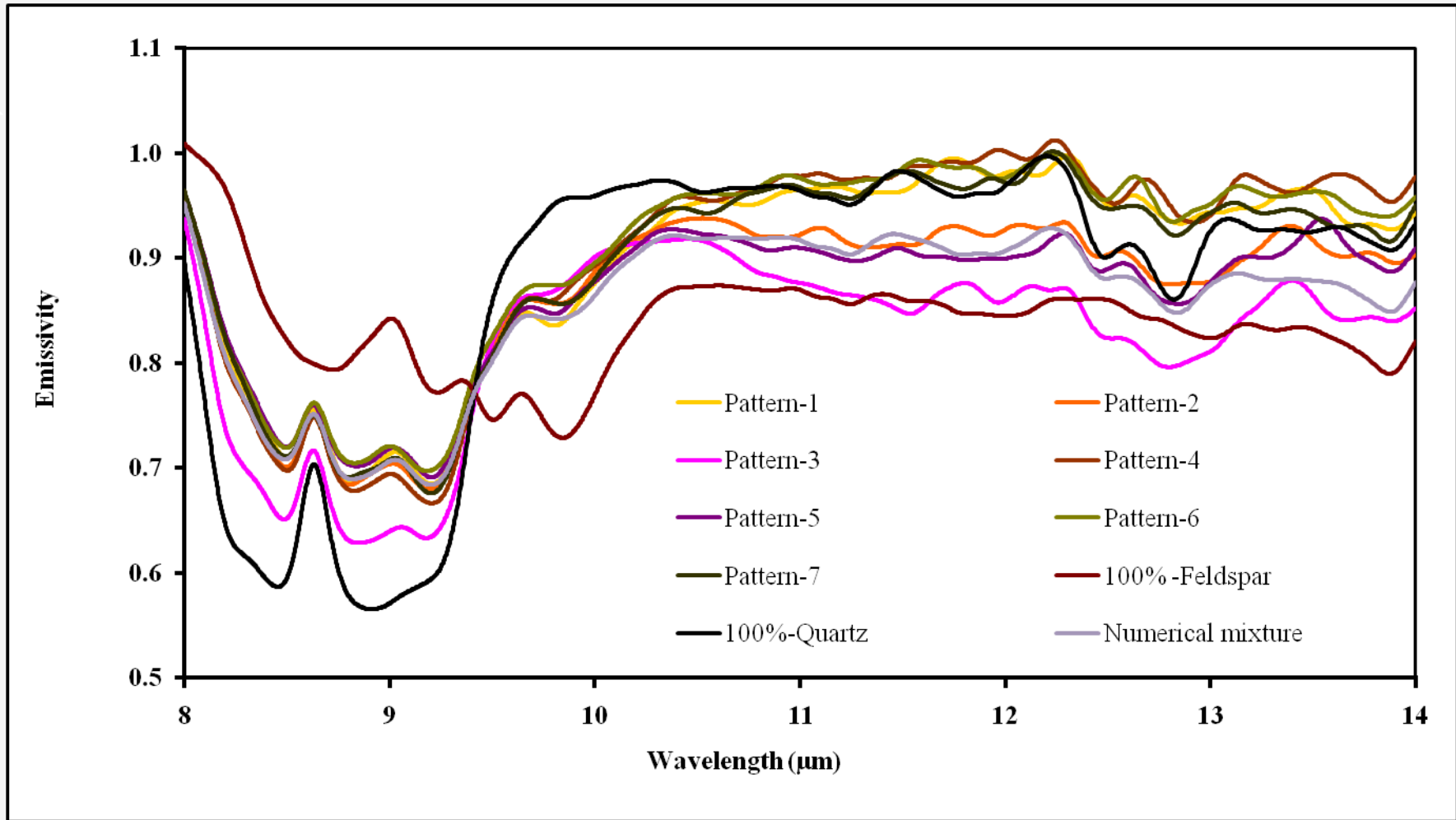


Quartz-Amphibole (50:50)



Effect of Fabric on IR-spectra (Q-F)

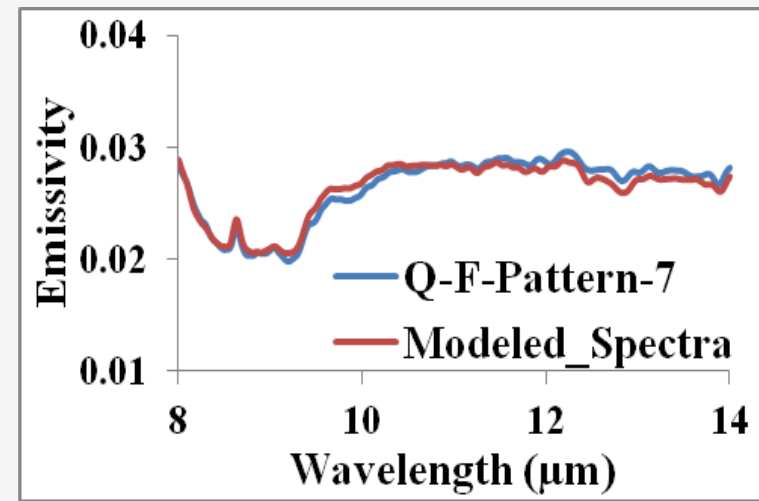
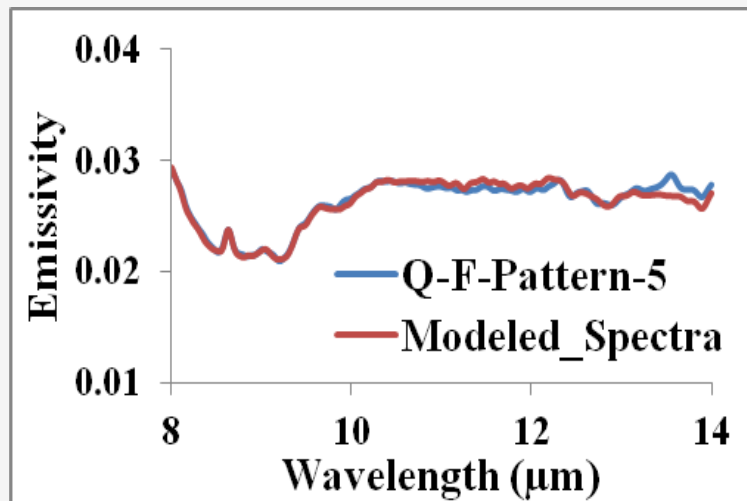
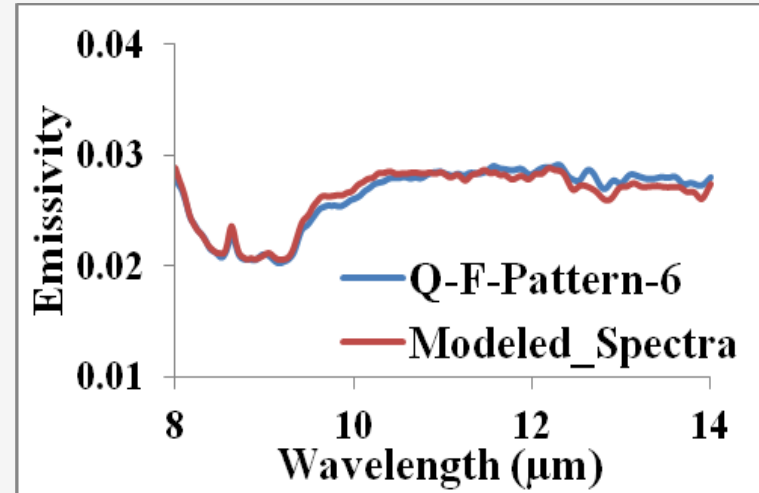
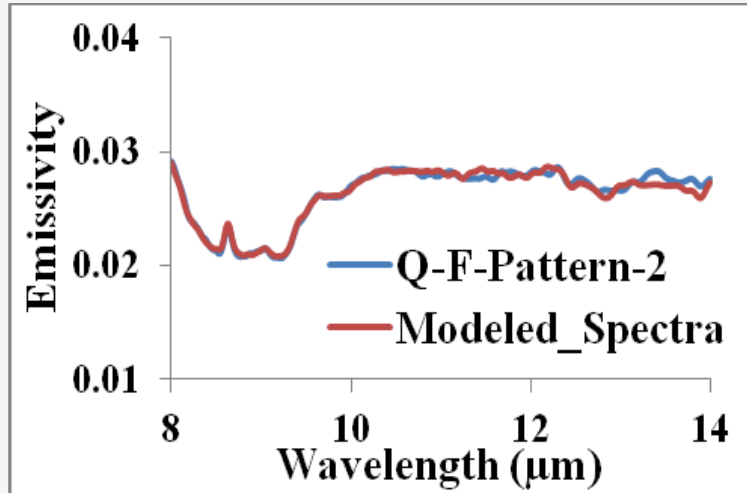
Variation in absorption feature



Quartz- Feldspar (50:50)



LMM: Two Component System (Q-F)





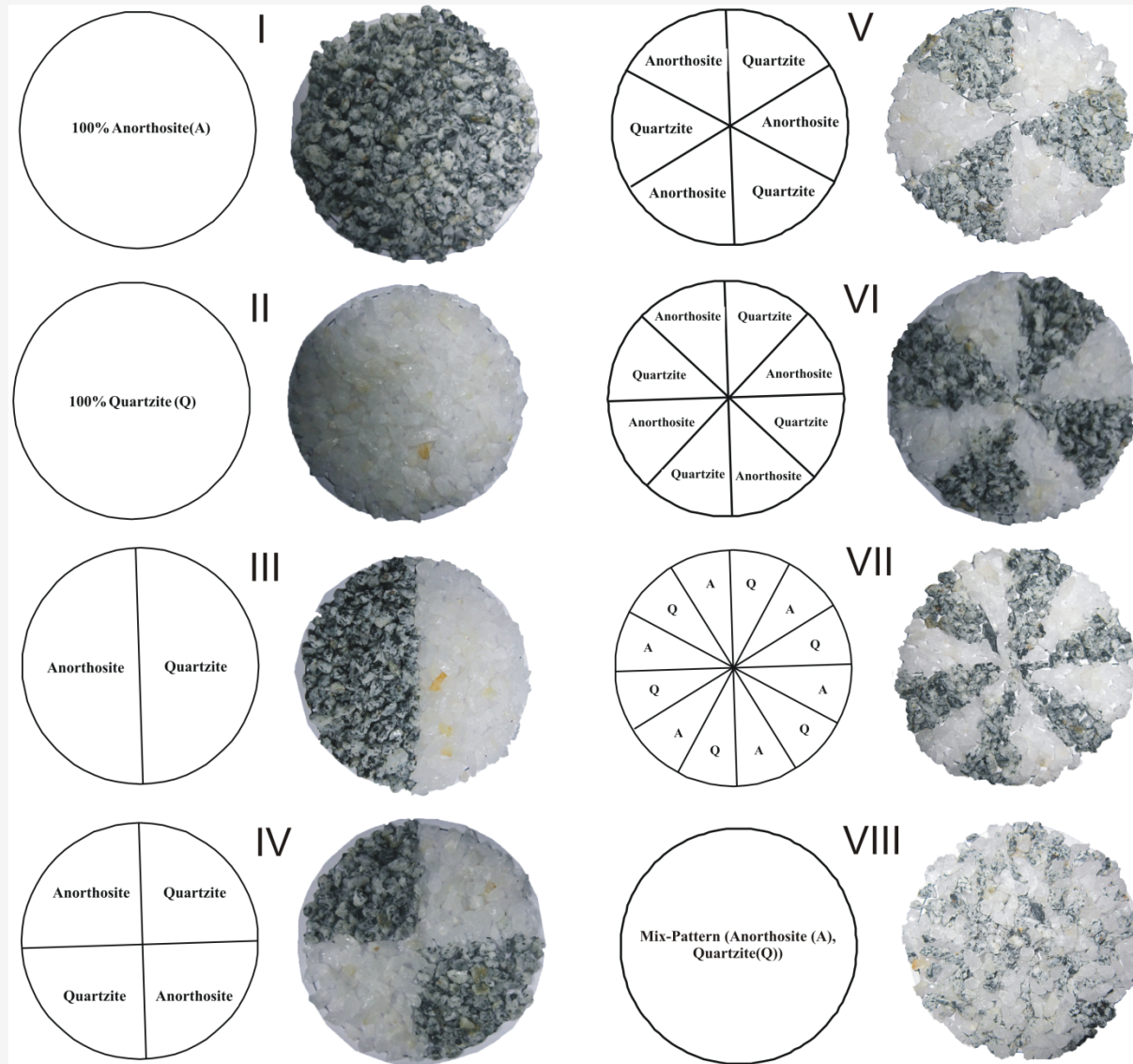
Comparison b/w Estimated and Actual Abundances



Pattern	RMSE	SAM Score	Estimated Abundance (%)	Actual Abundance (%)
1	0.0007	0.97	Q- 58.1, F- 42.3	Q- 50, F- 50
2	0.0003	0.99	Q- 55.0, F- 45.9	Q- 50, F- 50
3	0.0008	0.97	Q- 63.6, F- 36.8	Q- 50, F- 50
4	0.0008	0.97	Q- 65.0, F- 35.5	Q- 50, F- 50
5	0.0004	0.98	Q- 47.5, F- 53.0	Q- 50, F- 50
6	0.0006	0.98	Q- 59.0, F- 41.5	Q- 50, F- 50
7	0.0006	0.97	Q- 58.4, F- 42.0	Q- 50, F- 50

Two Component Rock System (A-Q)

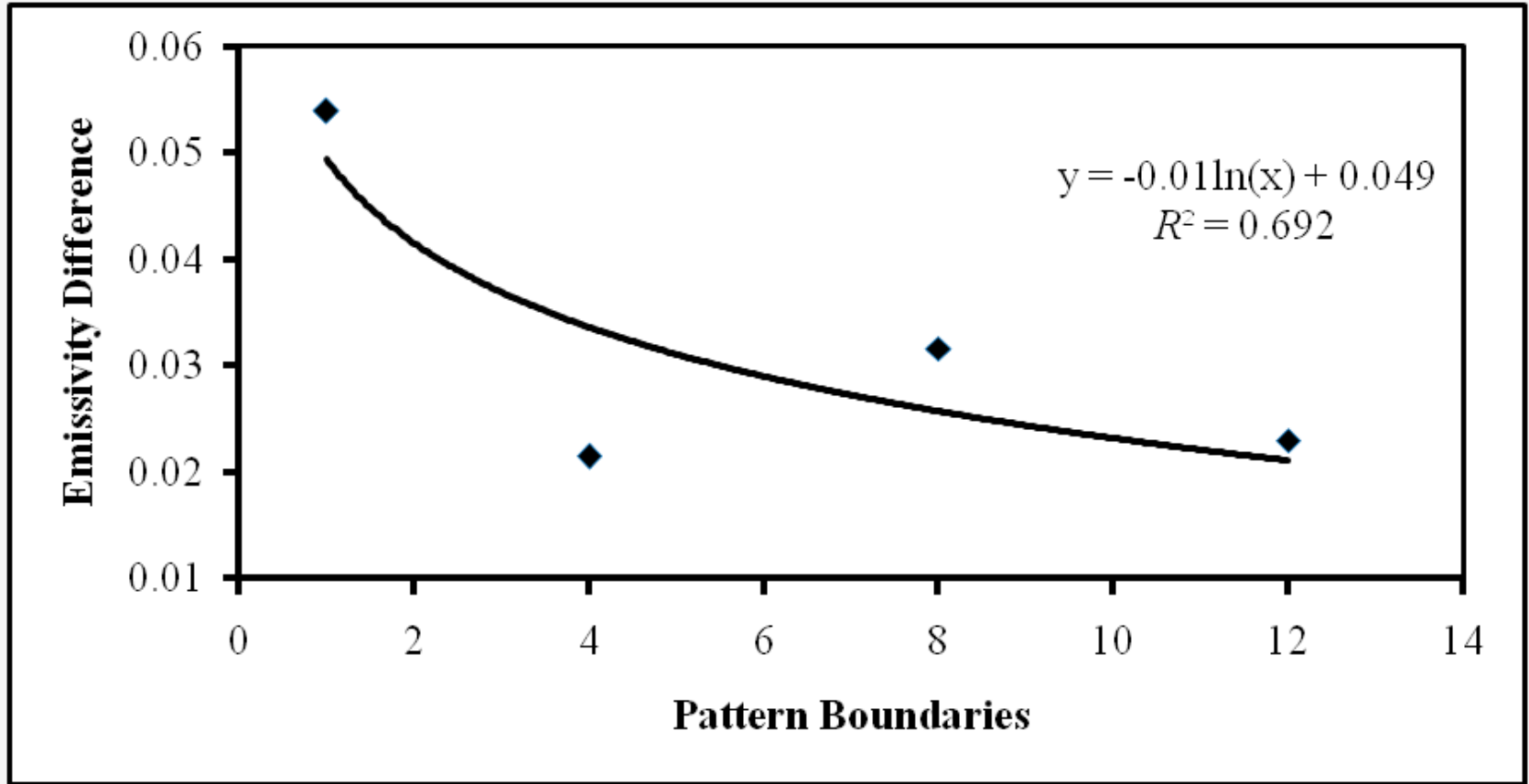
Two Component Rock System (A-Q) (2.36–4mm)



Patterns III, IV, V, VI, and VII have 1, 4, 6, 8 and 12 interface boundaries

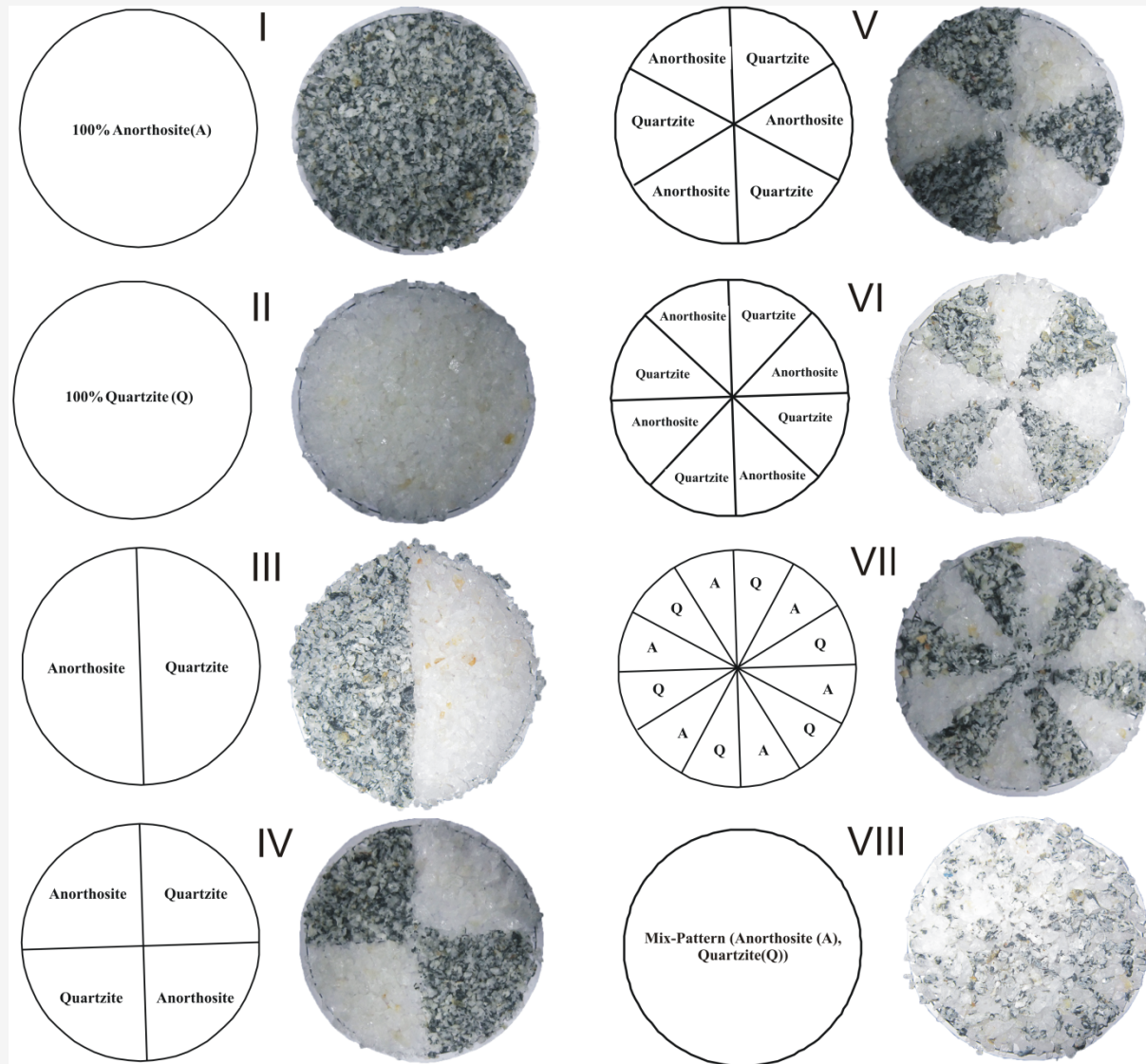


Scatter plot: Coarse Grain (2.36–4mm)



- Reststrahlen feature of Quartz (8.63μm) chosen to depict the non-linear effect on absorption feature
- Average emissivities at 8.63μm: 0.854 (theoretical) << 0.882 (measured)
- The density, grain size and fabric's emissivity are coupled with texture boundaries
- Variation in emissivity differences (measured and theoretical) *vis-a-vis* texture-fabric combinations (III-VII)

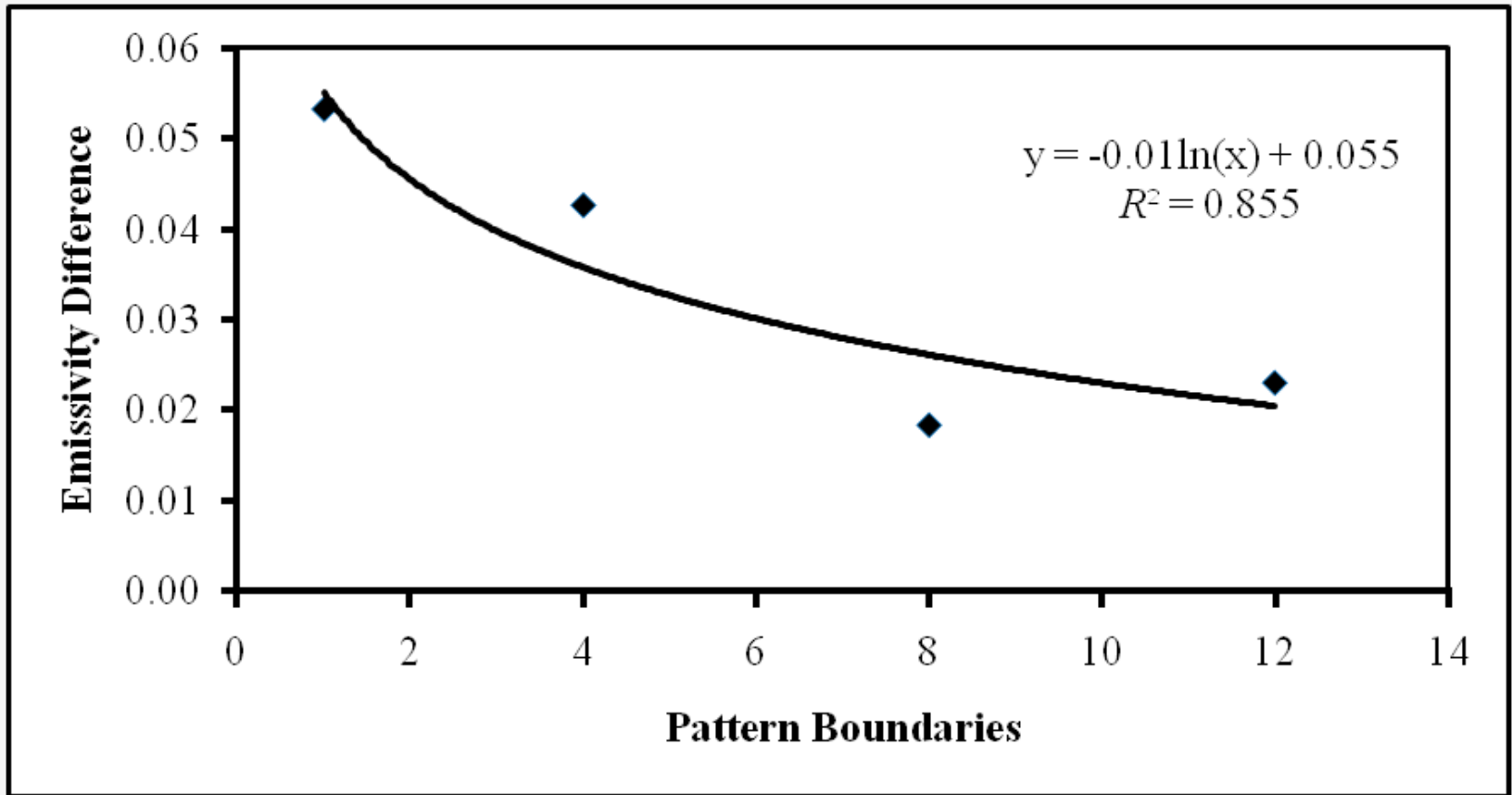
Two Component Rock System (A-Q) (1–2.36mm)



Patterns III, IV, V, VI, and VII have 1, 4, 6, 8 and 12 interface boundaries



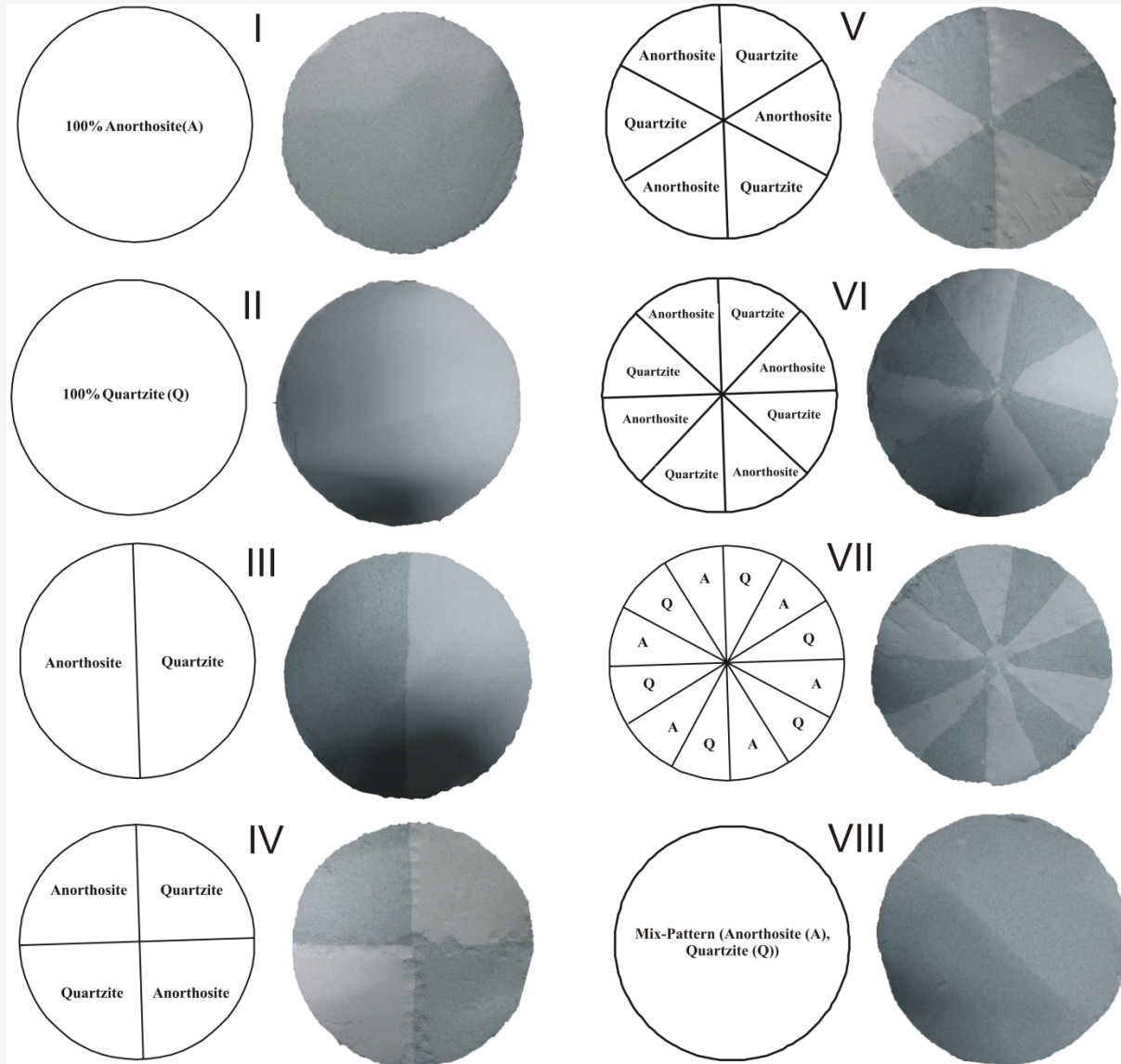
Scatter Plot: Medium Grain (1–2.36mm)



Average emissivities at $8.63\mu\text{m}$: 0.858 (theoretical) \ll 0.888 (measured)



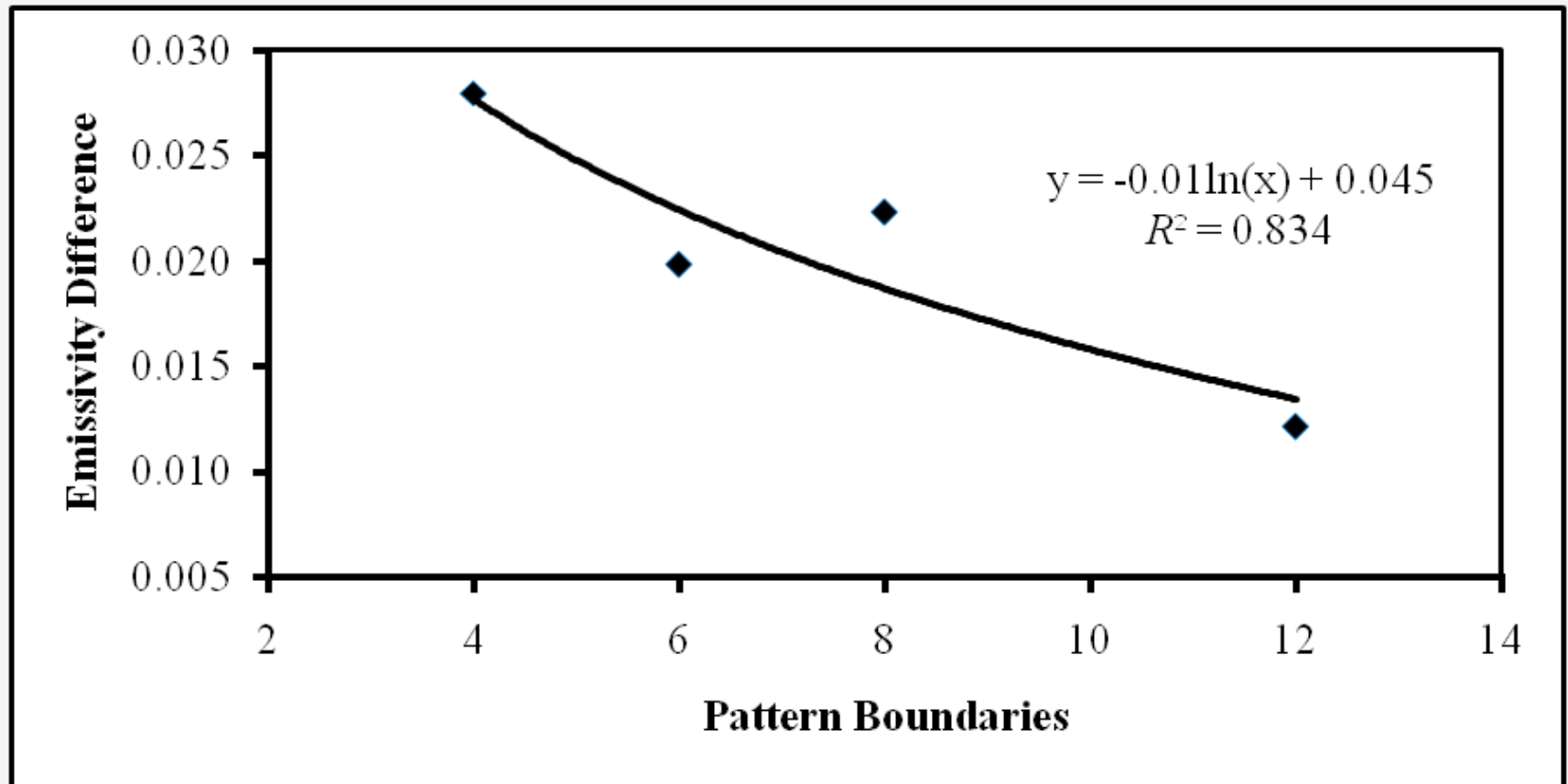
Two Component Rock System (A-Q) ($\leq 75\mu\text{m}$)



Patterns III, IV, V, VI, and VII have 1, 4, 6, 8 and 12 interface boundaries



Scatter plot: Fine Grain ($\leq 75\mu\text{m}$)

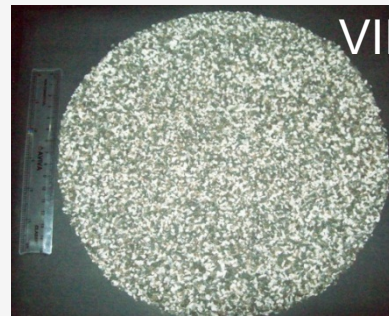
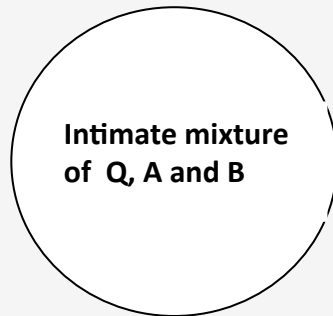
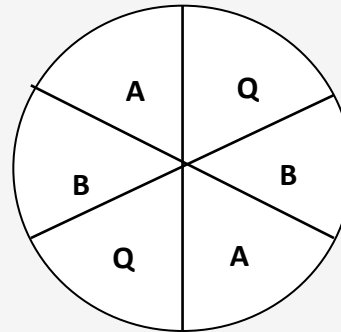
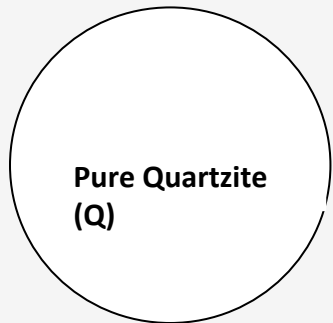
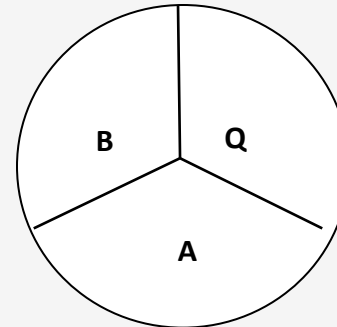
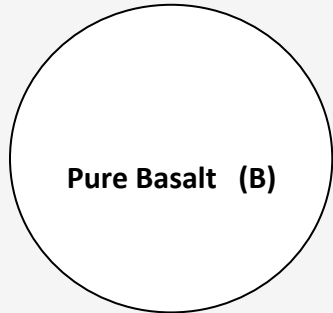
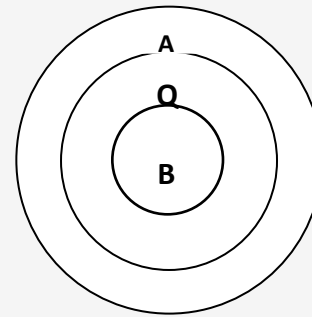
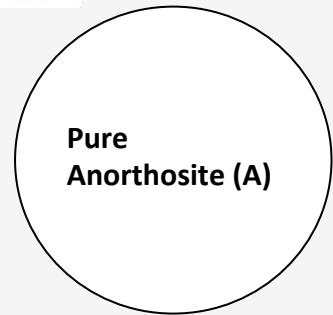


Average emissivities at $8.63\mu\text{m}$: 0.928 (theoretical) \ll 0.948 (measured)

Three Component Rock System (A-B-Q)



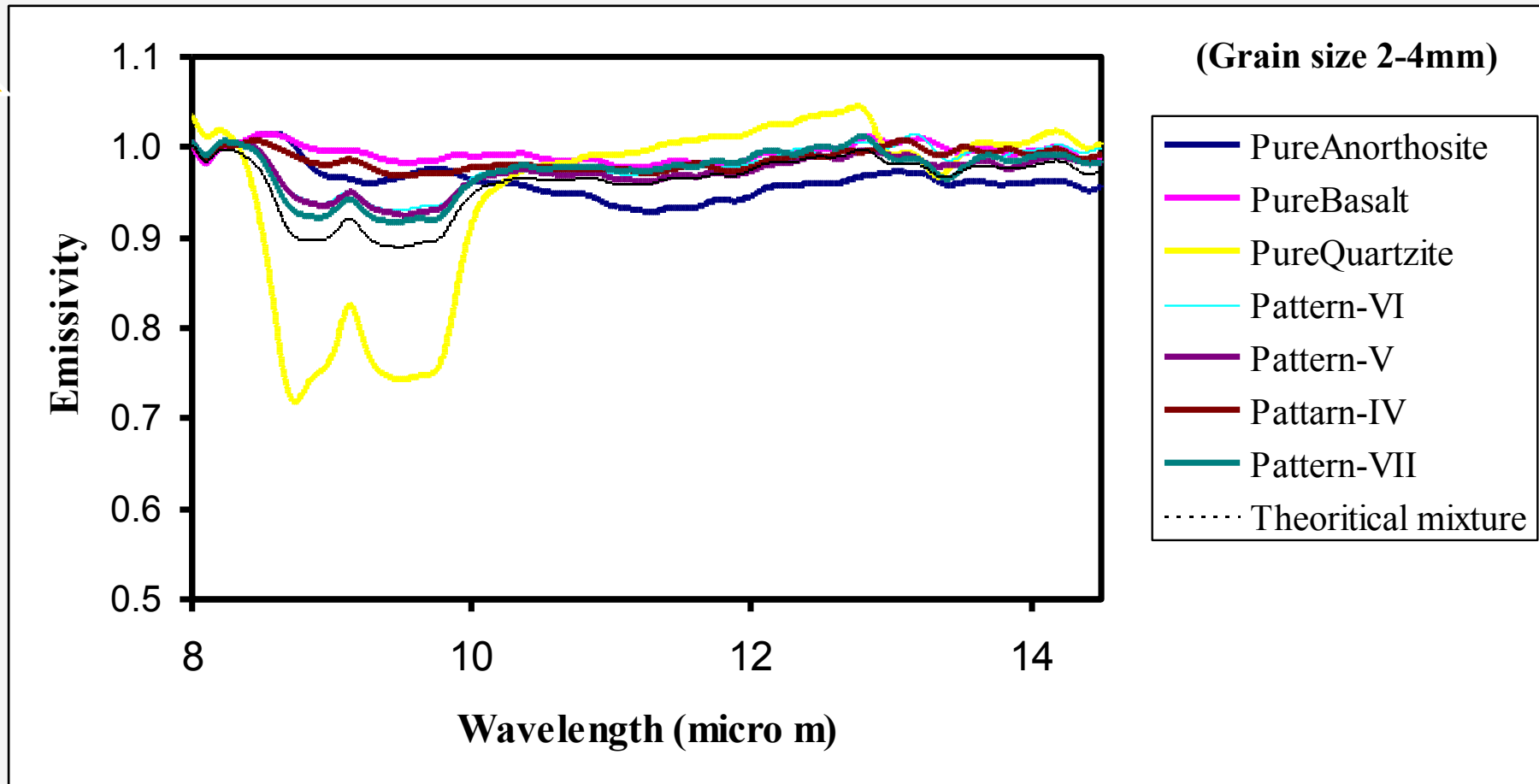
Sample Patterns: Three Component System



3 Samples (A, B, Q):
 1134 combinations
 (3 textures x 7 fabrics
 x 54 geometry)



Effect of Fabric on IR-spectra (B-A-Q)

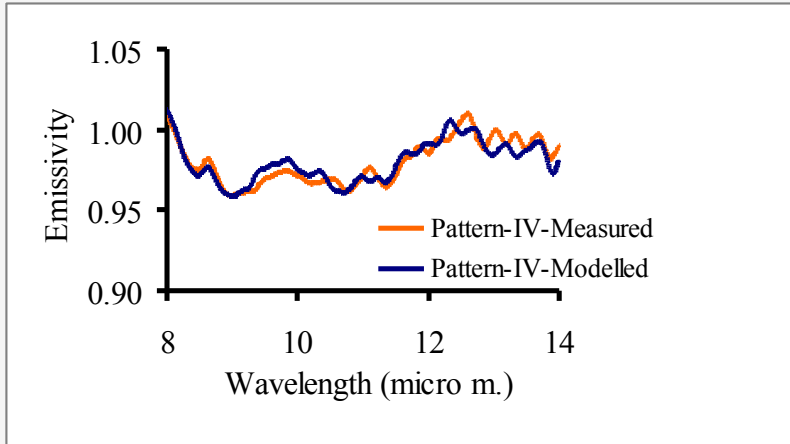


Pattern Mixture: Basalt-Anorthosite-Quartzite (33:33:33)

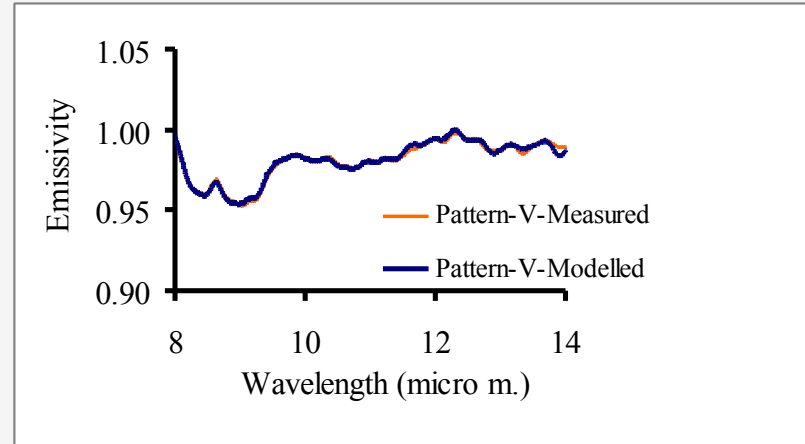


LMM- Three Component System (B-A-Q)

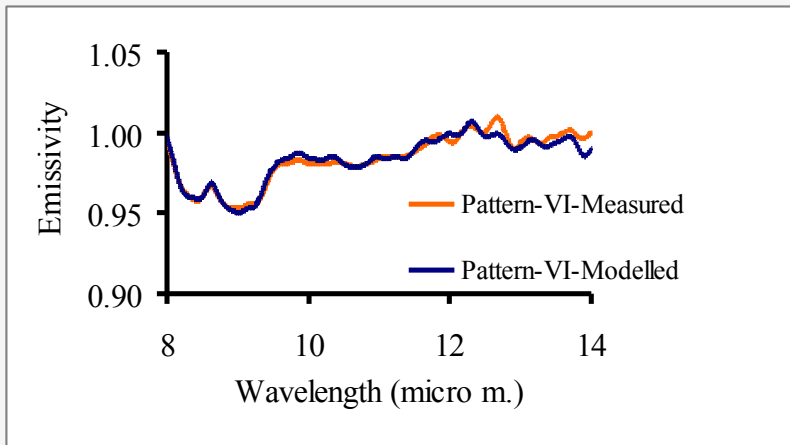
Pattern-IV



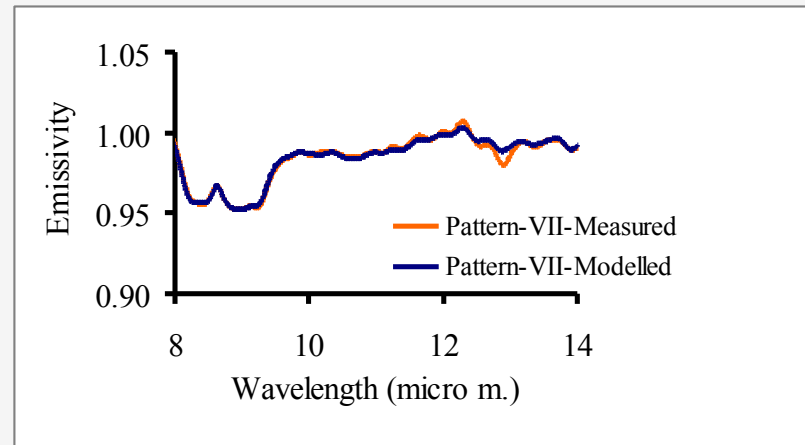
Pattern-V



Pattern-VI



Pattern-VII

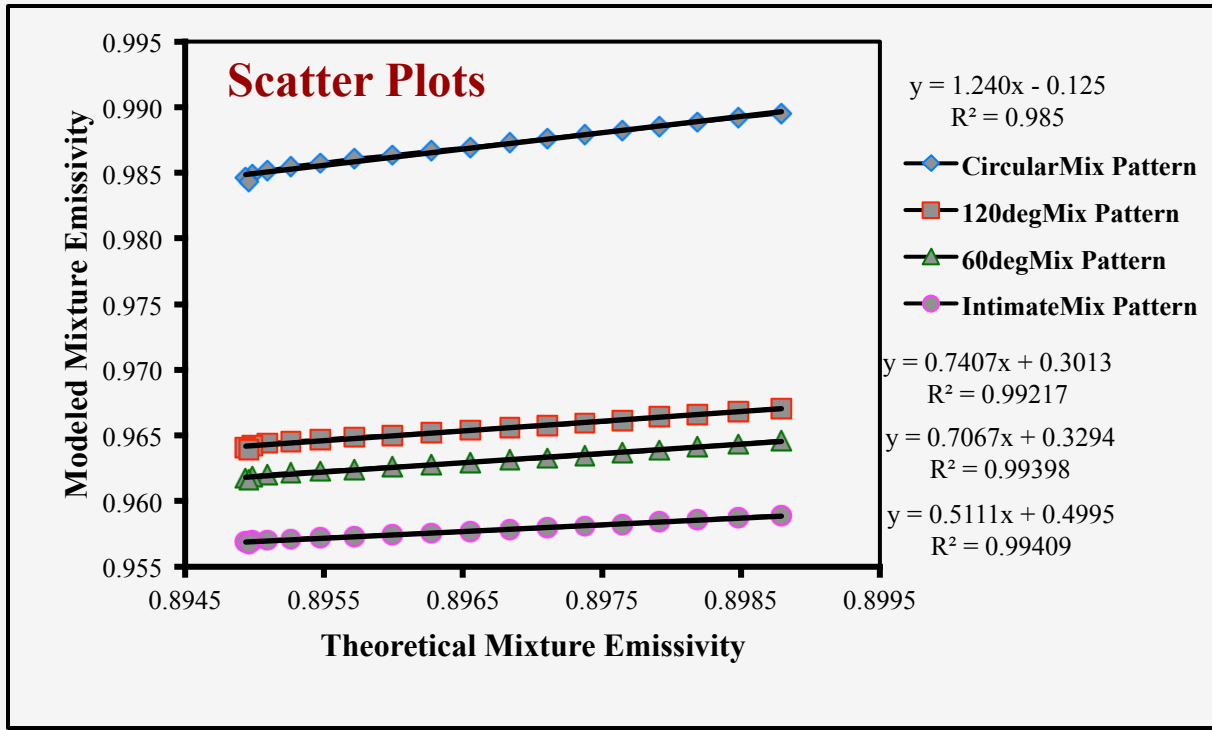




Estimated Pattern Abundances

Pattern	Estimated Abundance (%)	RMSE	SAM Score
IV	Basalt– 33.0, Anorthosite– 36.0, Quartzite– 31.0	0.0043	0.82
V	Basalt– 34.4, Anorthosite– 8.8, Quartzite– 56.8	0.0061	0.75
VI	Basalt– 18.4, Anorthosite– 18.2, Quartzite– 63.4	0.0051	0.79
VII	Basalt– 23.1, Anorthosite– 6.0, Quartzite– 70.9	0.0042	0.83

Statistical Evaluation (R^2 and F -test): $\lambda_1 \sim 8.21-8.25\mu\text{m}$

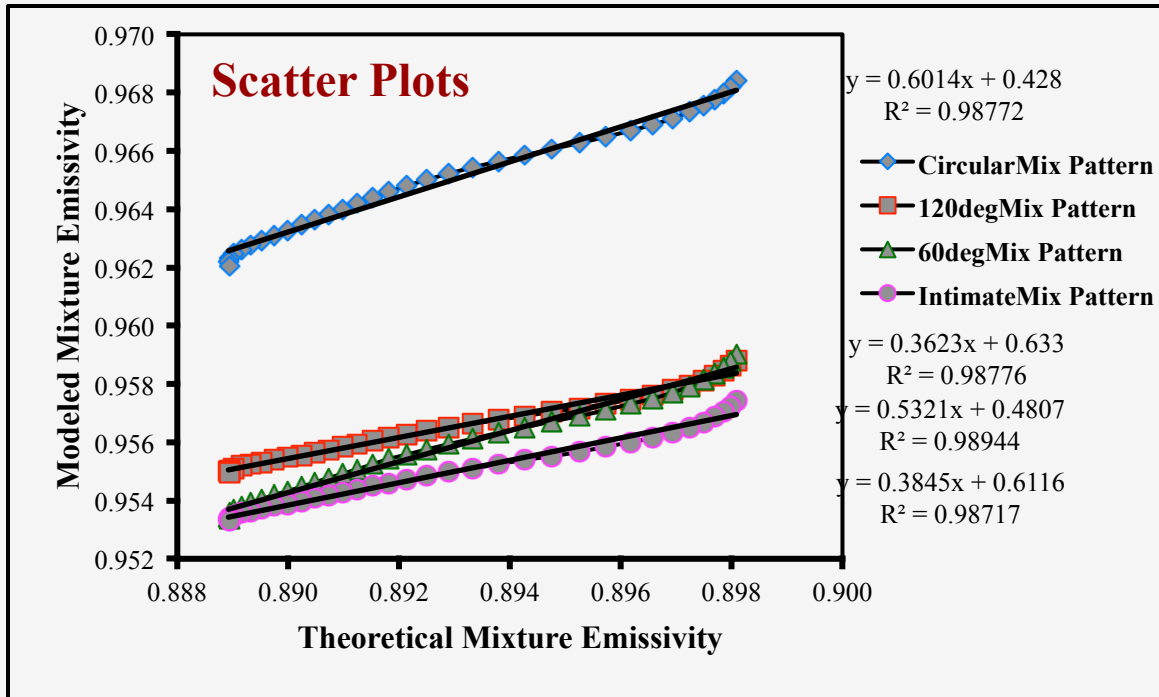


Samples: Anorthosite, Basalt and Quartzite
Grain Size: 2-4mm
Patterns: IV, V, VI, VII
First major absorption feature (λ_1): 8.21-8.25 μm
F-values \gg F-critical: Results are significant
Result: fabric-texture related multiple scattering

Statistical Relationship

Statistical Parameters	Mixture Patterns			
	CircularMix Pattern	120degMix Pattern	60degMix Pattern	IntimateMix Pattern
<i>Regression coefficient (R^2)</i>	0.985	0.992	0.994	0.994
<i>Total degree of freedom (df)</i>	16	16	16	16
<i>F-distribution (estimated)</i>	0.624	1.803	2.008	3.912
<i>F-critical (F_c)</i>	0.296	1.778	1.988	3.372
<i>Significance (S)</i>	99%	87%	91%	99%

Statistical Evaluation (R^2 and F -test): $\lambda_2 \sim 8.75-8.84\mu\text{m}$



Samples: Anorthosite, Basalt and Quartzite
Grain Size: 2-4mm
Patterns: IV, V, VI, VII
Second major absorption feature (λ_2): 8.75-8.84 μm
F-values \gg F-critical:
 Results are significant

Result: fabric-texture related multiple scattering

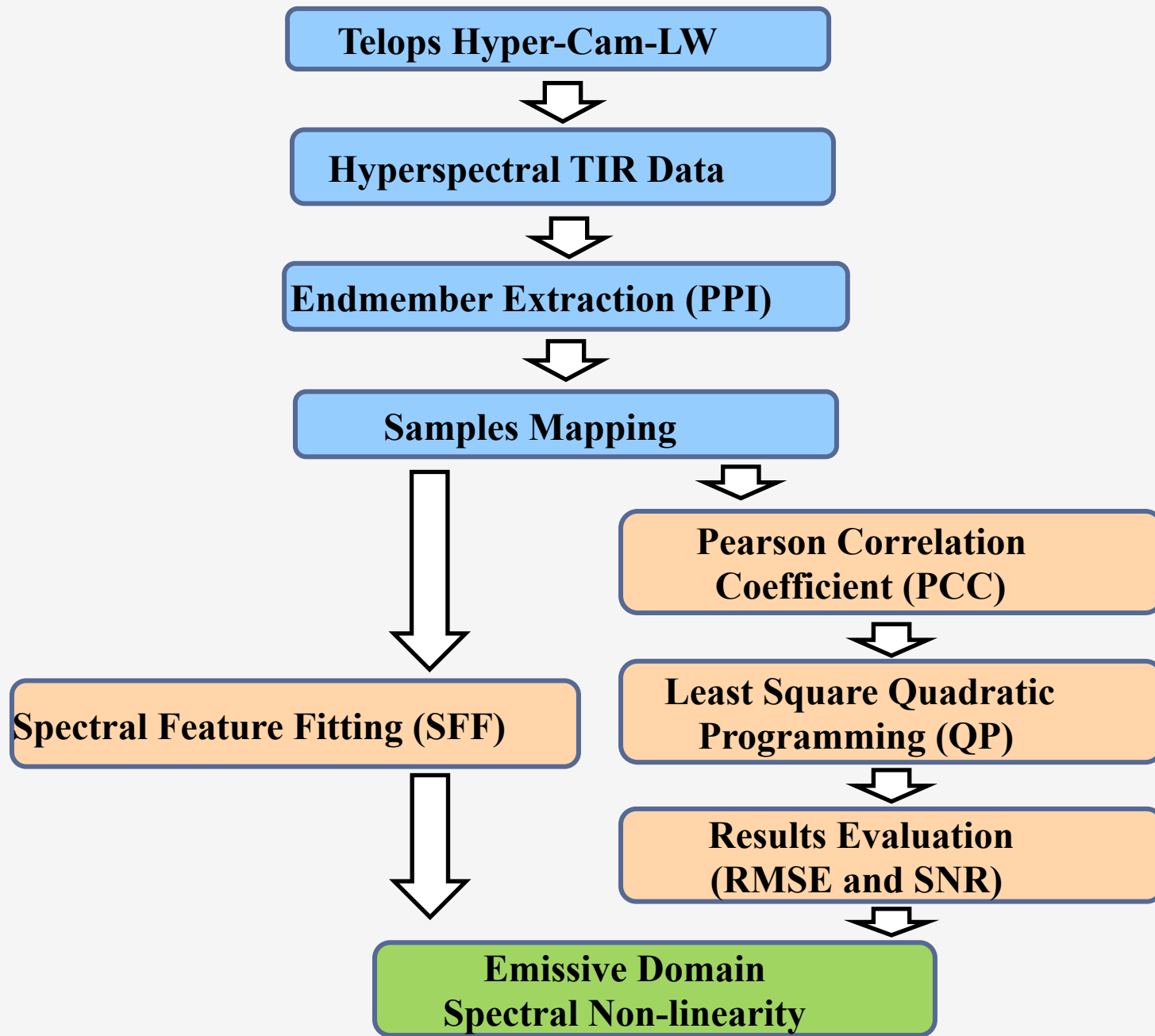
Statistical Relationship

Statistical Parameters	Mixture Patterns			
	CircularMix Pattern	120degMix Pattern	60degMix Pattern	IntimateMix Pattern
<i>Regression coefficient (R^2)</i>	0.987	0.987	0.989	0.987
<i>Total degree of freedom (df)</i>	32	32	32	32
<i>F-distribution (estimated)</i>	2.775	7.860	3.597	6.978
<i>F-critical (F_c)</i>	2.095	2.318	2.095	2.318
<i>Significance (S)</i>	98%	99%	98%	99%

Uncertainties in TIR Hyperspectral Image Cube Unmixing (Telops IR-Hypercube)

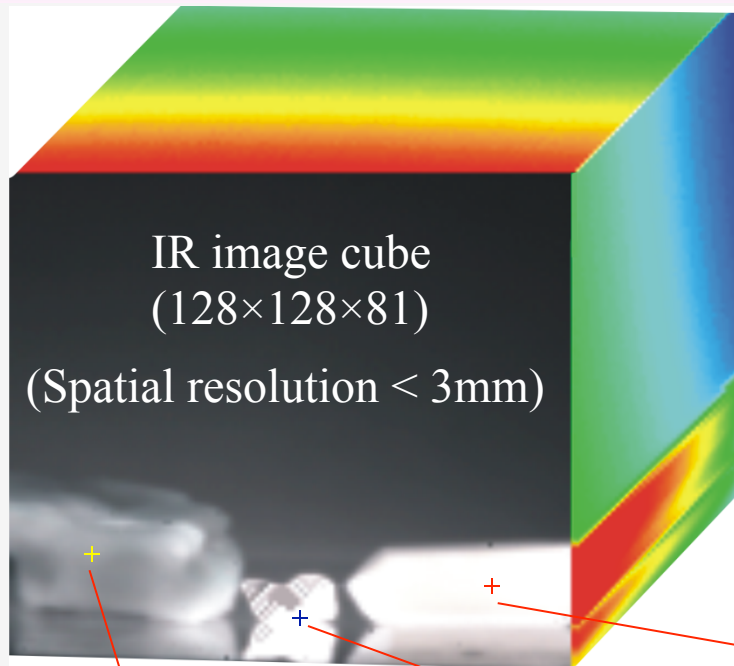


Processing and Analysis Steps:

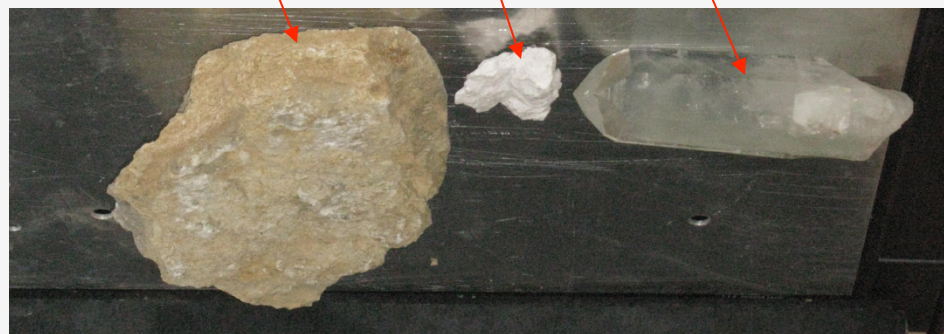




Telops Hyperspectral Image Cube



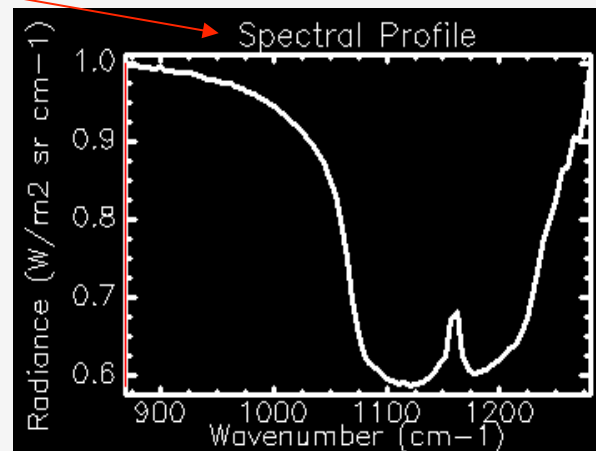
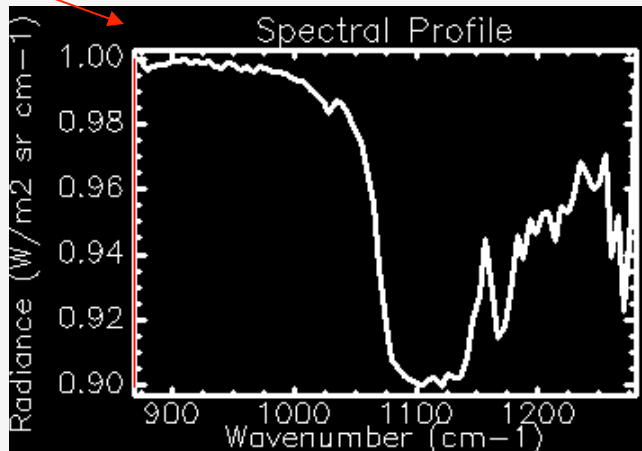
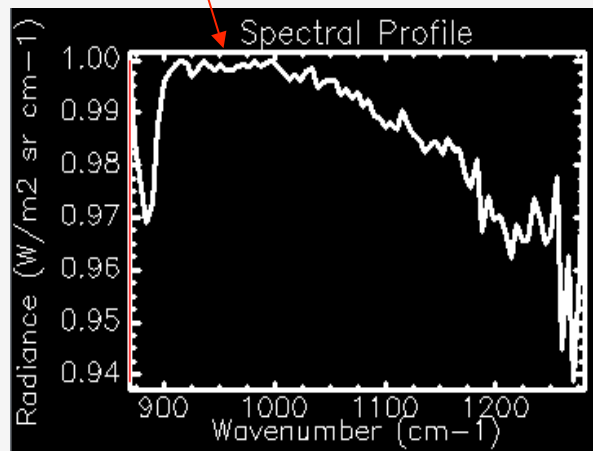
Limestone Alunite Quartz



Wavelength : 8-12 μm

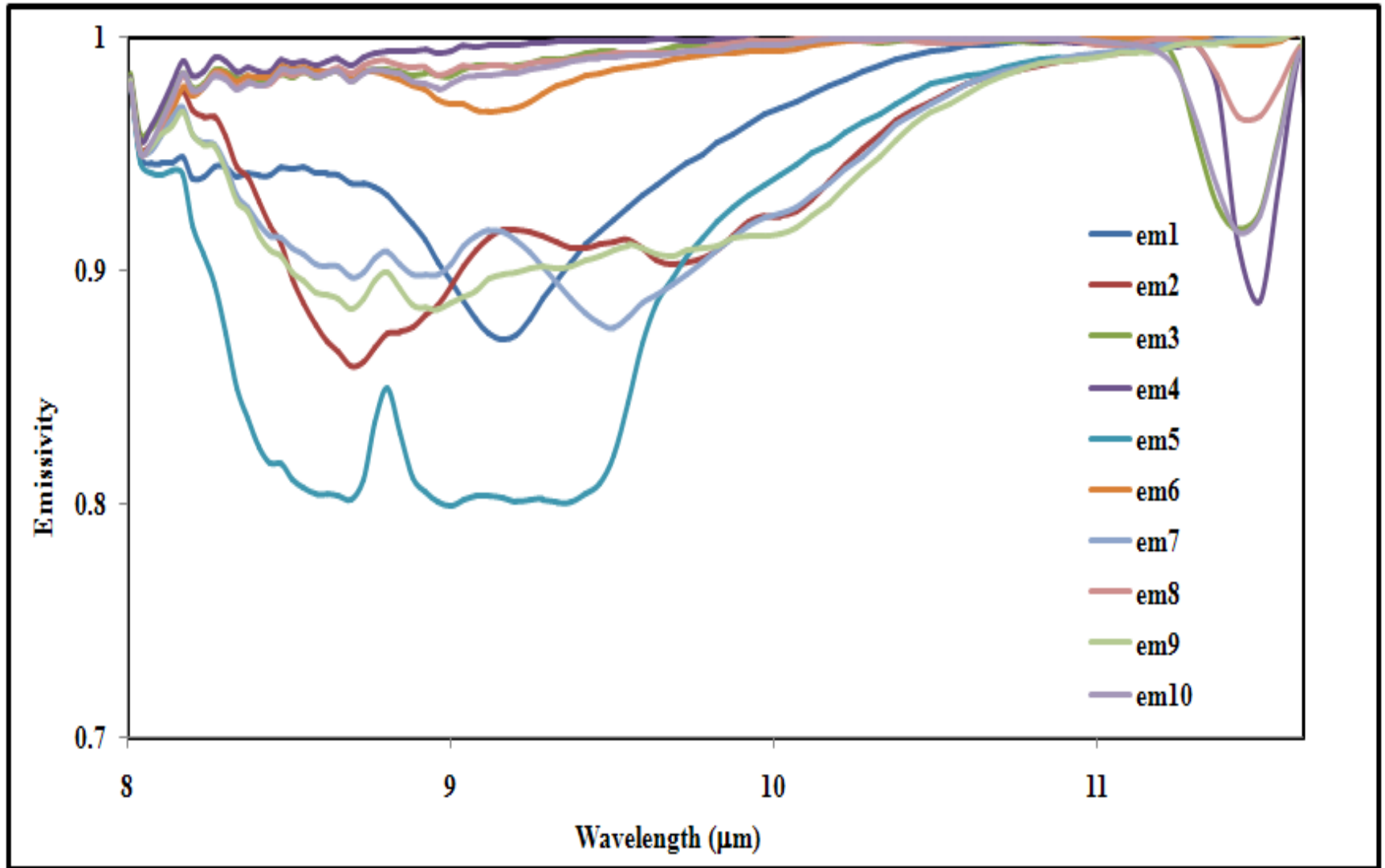
No. of bands: 81

Spectral resolution: 0.25 to 150 cm^{-1}

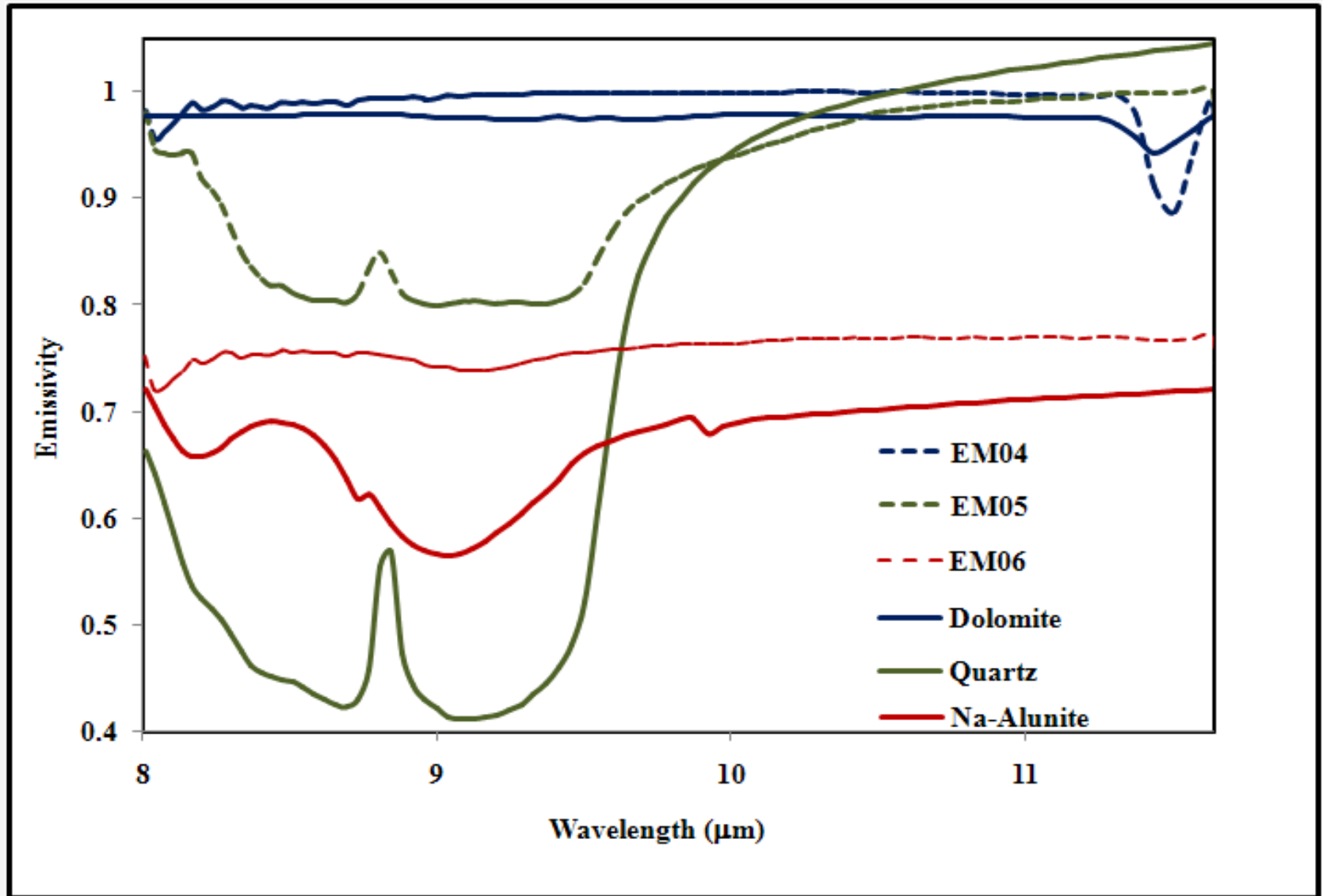




Hypercube Endmembers (using PPI)



Endmembers Spectra and Library Counterparts

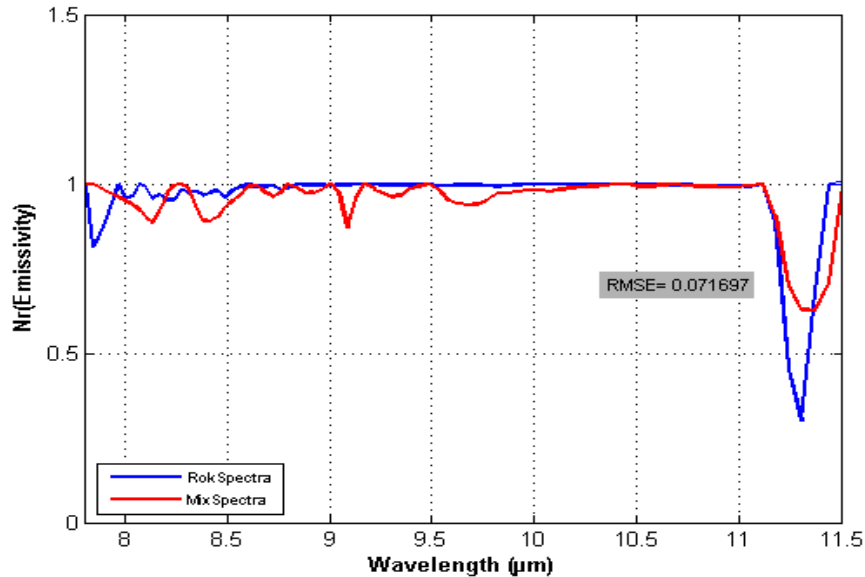


Other EMs are spectral mixtures of these three minerals

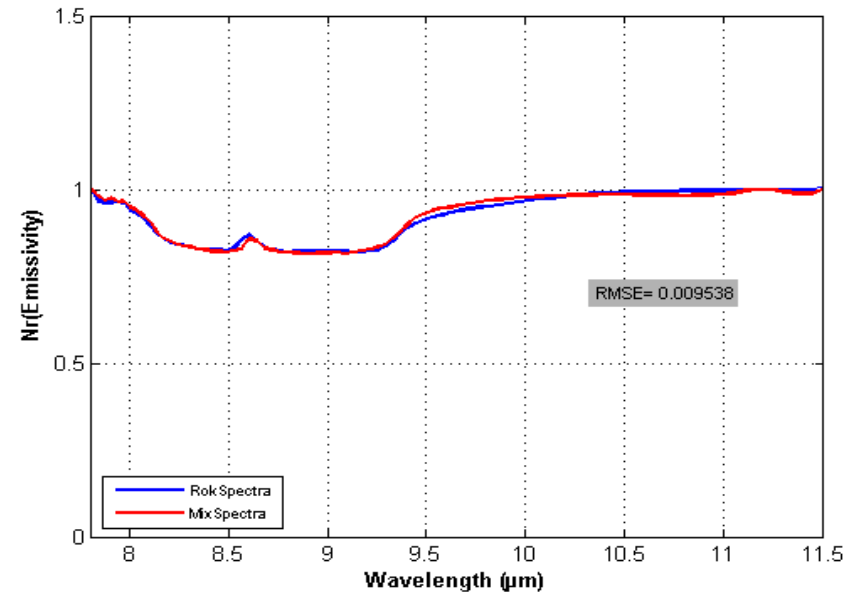


Image Endmembers vs. Modeled Spectra

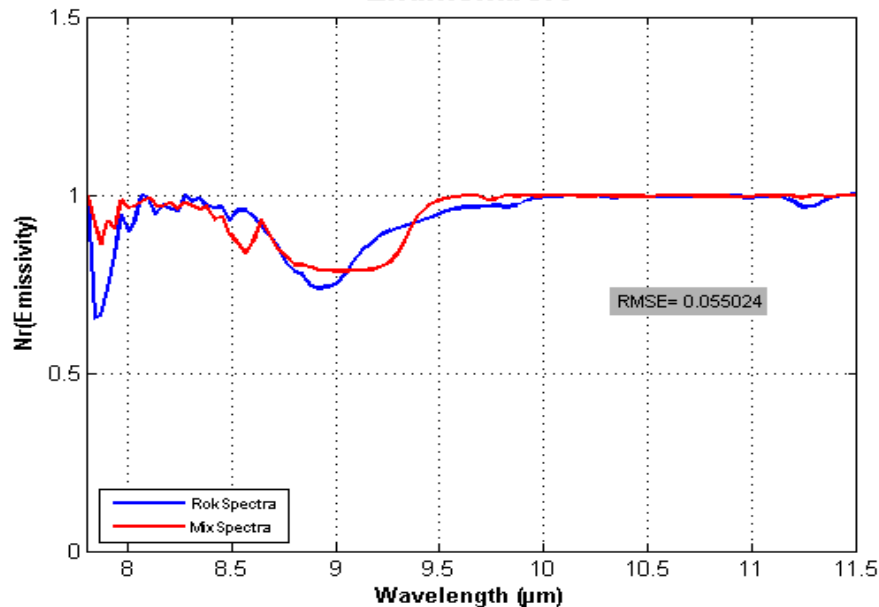
Endmember4



Endmember5



Endmember6



- These **EMs** are transformed and compared with JHU library mineral spectra (using PCC) and subsequent unmixed (by LMM)
- **EM04 (Limestone):** 100% Dolomite ($\text{Ca-Mg}(\text{CO}_3)_2$)
- **EM05 (Quartz):** 100% Quartz (SiO_2)
- **EM06 (Alunite):** 100% Na-alunite ($\text{NaAl}_3(\text{SO}_4)_2(\text{OH})_6$)

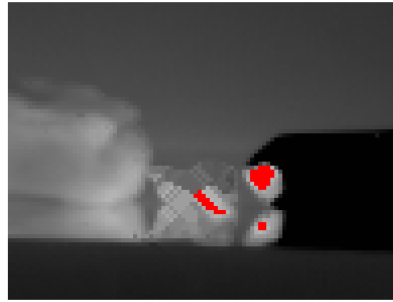


Mineral Abundances of Image Endmembers

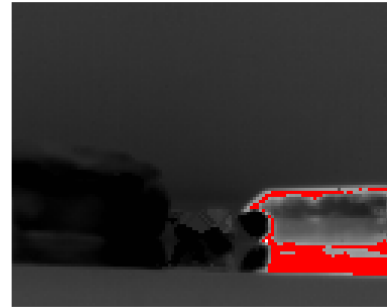
Image Endmembers	Mineralogy (%)	RMSE	SAM Score
EM01	Quartz : 39% Alunite: 49% Dolomite: 12%	0.03	0.75
EM02	Quartz: 65% Calcite: 10% Dolomite: 25%	0.04	0.65
EM03	Dolomite: 90% Quartz: 10%	0.08	0.17
EM04	Dolomite: 100%	0.07	0.30
EM05	Quartz: 100%	0.01	0.91
EM06	Alunite: 100%	0.06	0.48
EM07	Quartz: 62% Dolomite: 38%	0.04	0.65
EM08	Alunite: 35% Dolomite: 65%	0.08	0.18
EM09	Quartz: 64% Calcite: 1% Dolomite: 35%	0.03	0.70
EM10	Dolomite: 90% Quartz: 5% Alunite: 5%	0.08	0.19



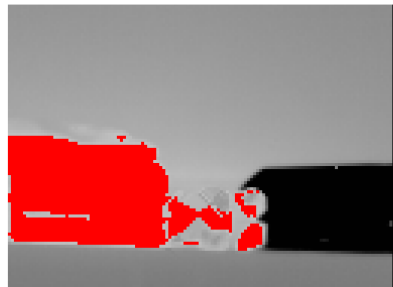
Classified Image Cube



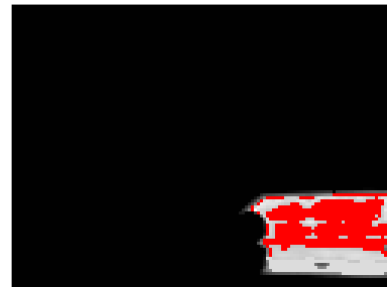
EM01



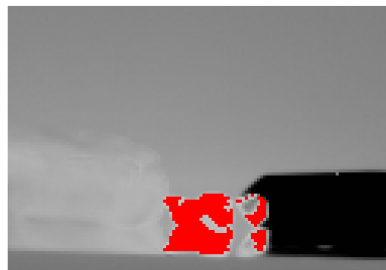
EM02



EM04



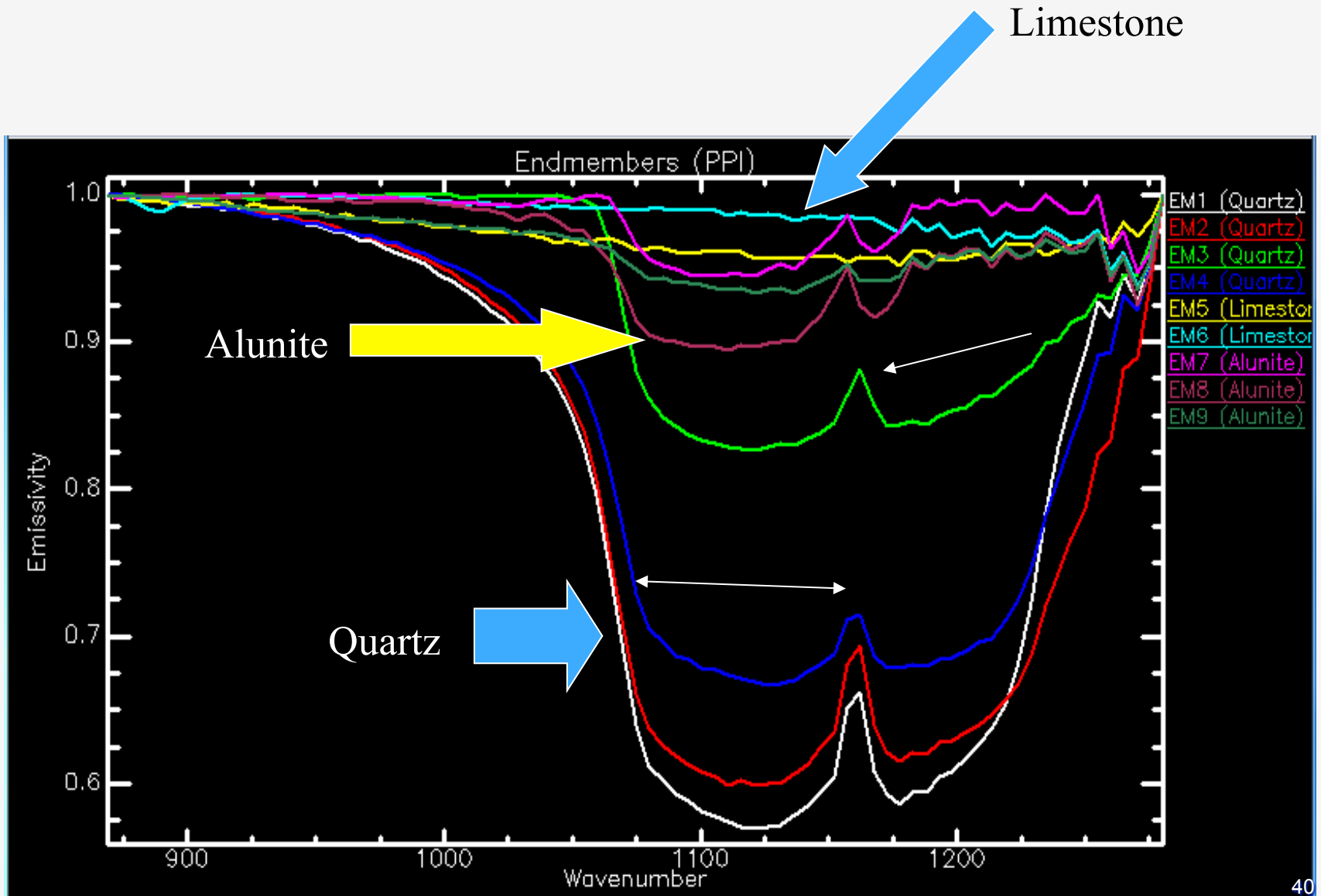
EM05



EM06



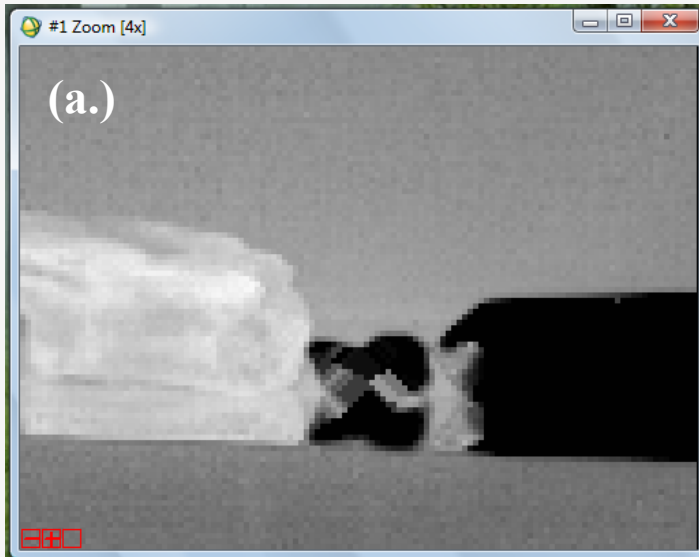
Image Endmember Spectra (using PPI)



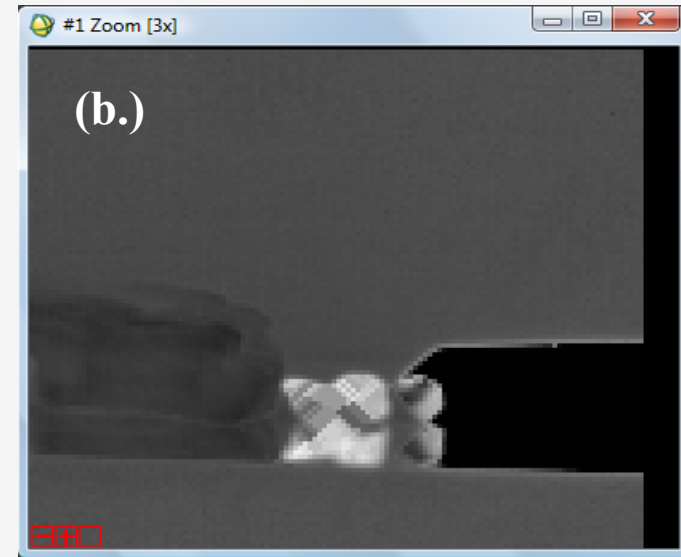


Mineral Mapping (using SFF)

Limestone Mapping



Alunite Mapping



Quartz Mapping

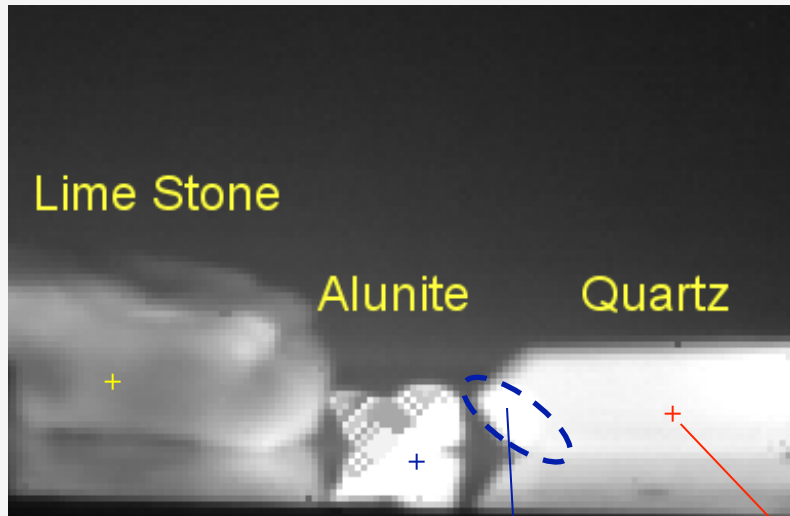


Image mapping of (a.) Limestone (b.) Alunite and (c.) Quartz using SFF.

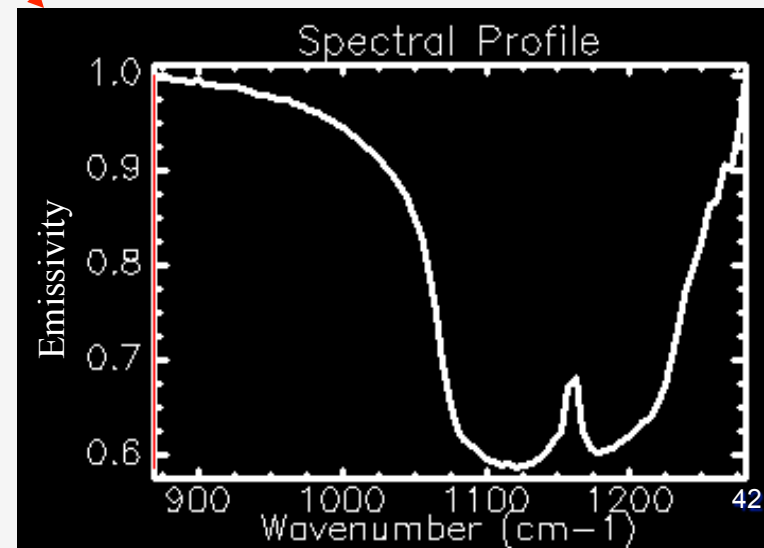
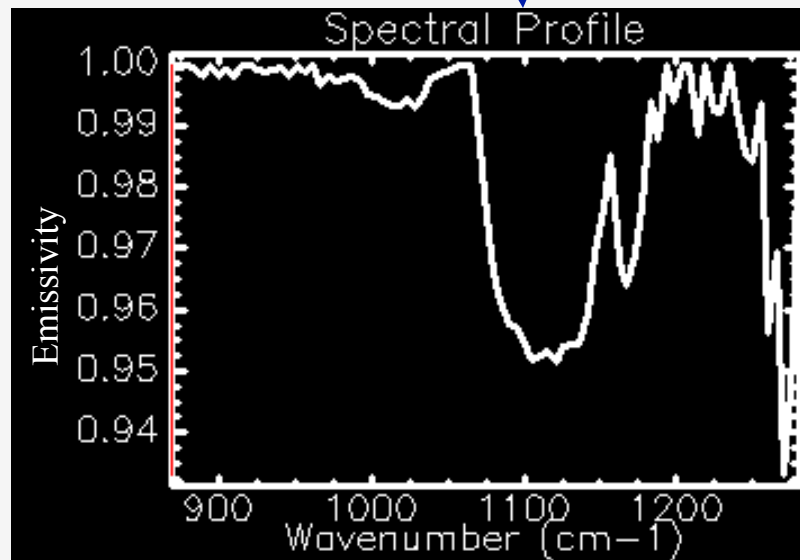
- limestone and alunite is completely mapped
- In image (b.) extreme left of the quartz crystal (light color pixels) mapped with mix-alunite and in (c.) the same area of the quartz sample remains unmapped.
- Caused by interaction of emitted energy



Causes of Uncertainty Zone

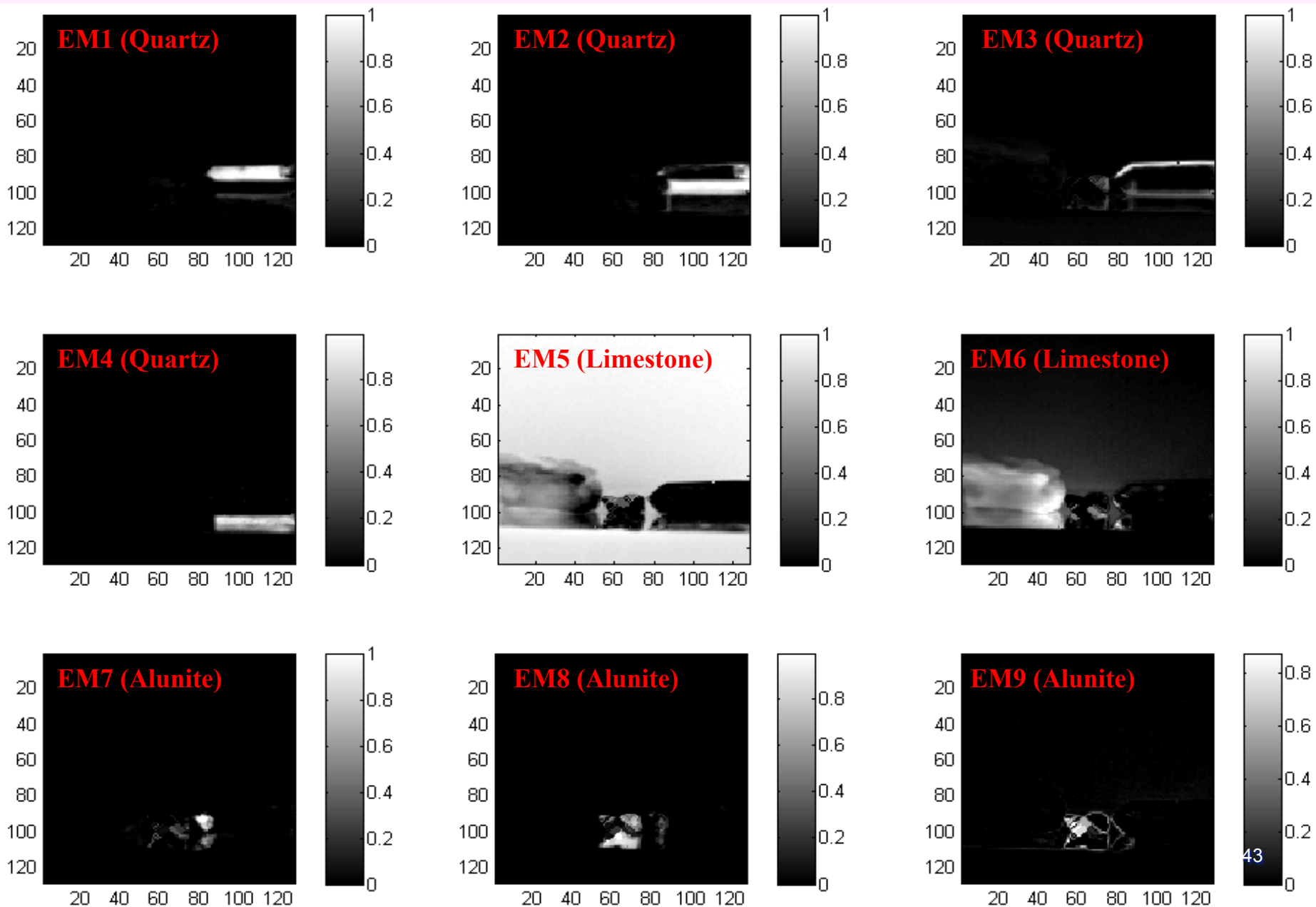


- Unmapped area (*dotted ellipse*) shows the higher uncertainty zone due to the dominance of alunite emissivity over quartz
- Coupling of Emitted Radiation: Radiation emitted by each material is absorbed/transmitted through the adjacent materials and then emitted towards the sensor
- Emission spectroscopy is clearly not a case of linear spectral mixing



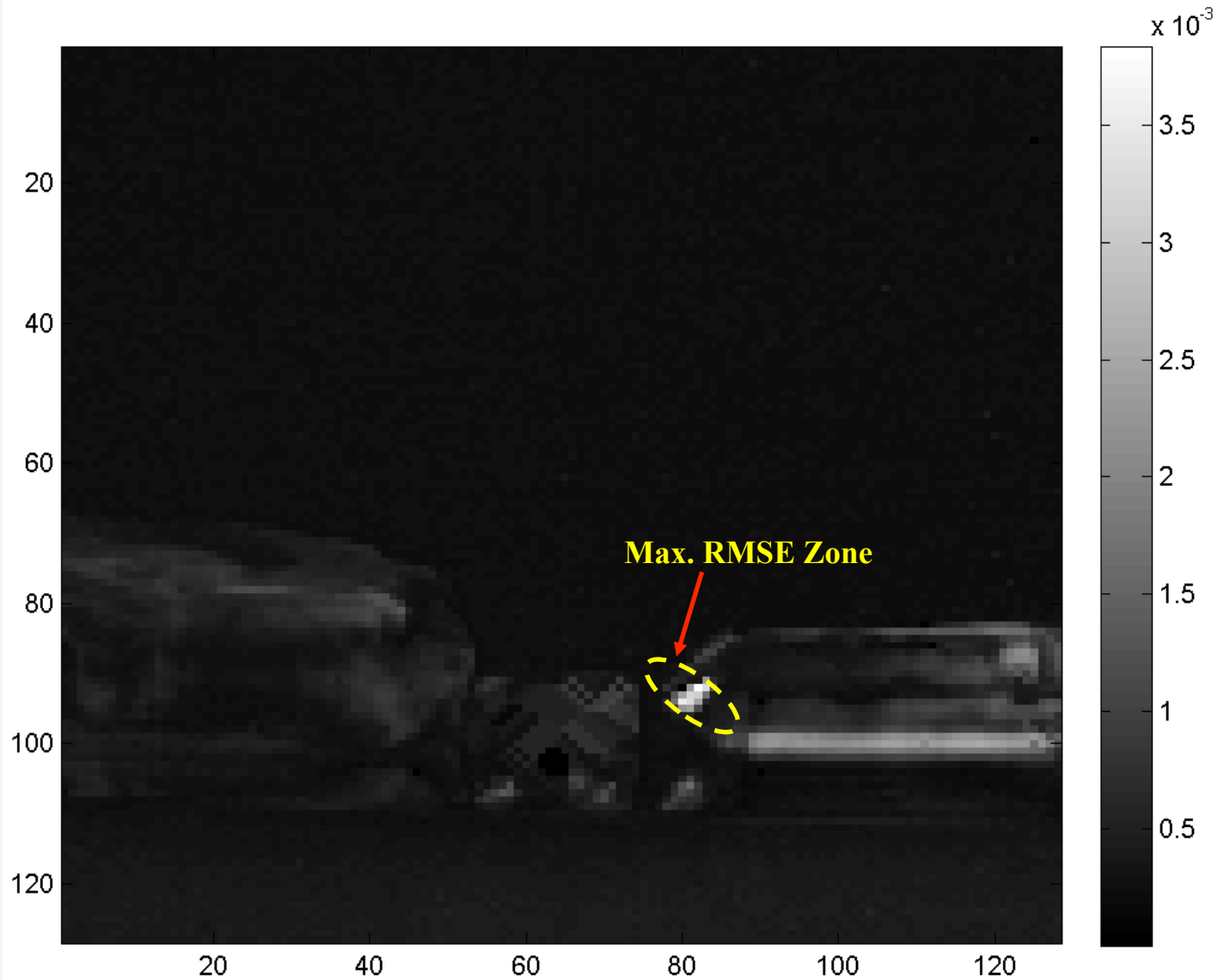


Abundance Maps (using FCLSE)



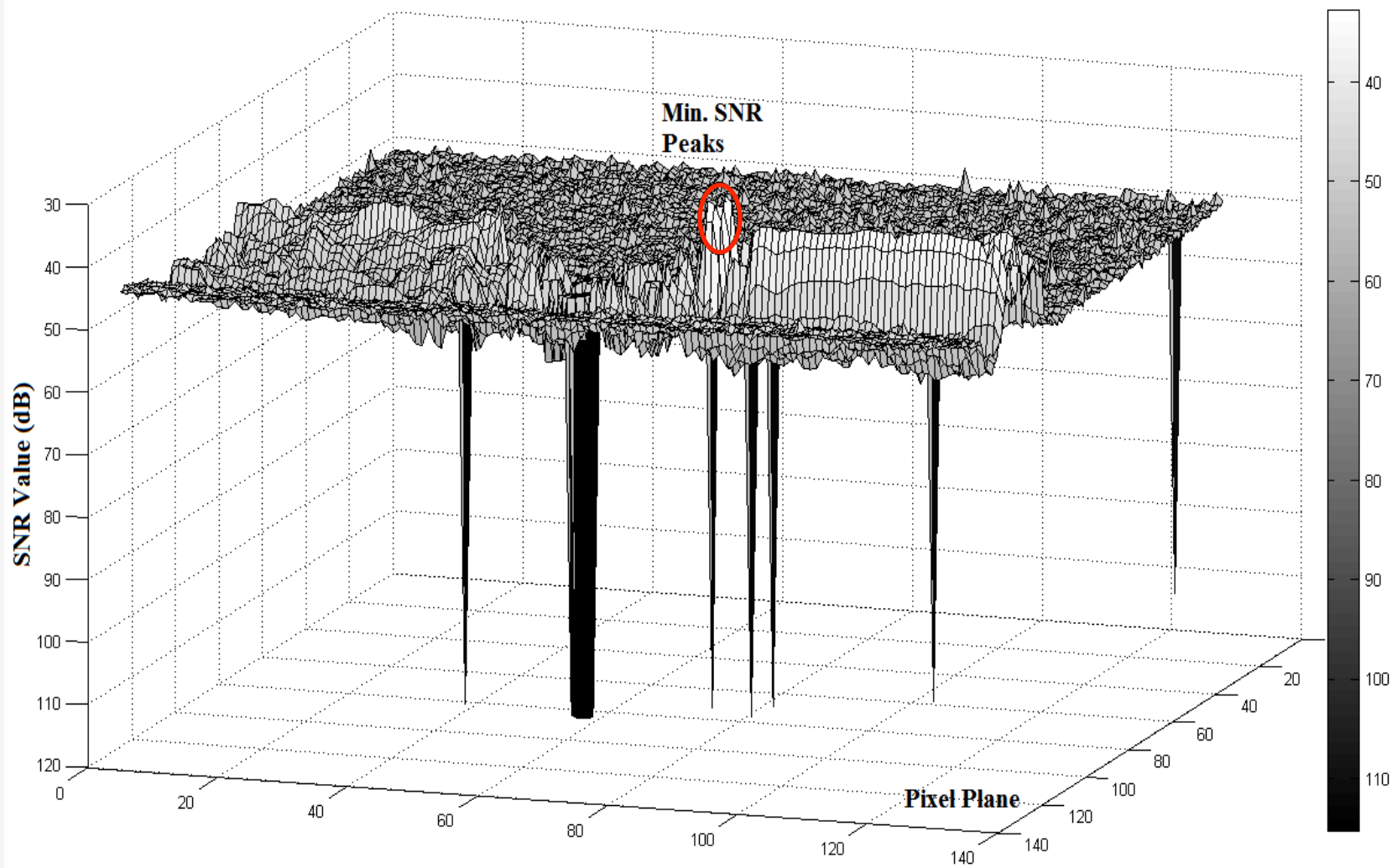


RMSE Value of each Image Pixel



RMSE Plane: RMS difference between actual and estimated modeled spectra for each image pixel. *Dotted ellipse* showing maximum RMSE zone. 44

Signal-to-Noise Ratio (SNR) of each Image Pixel



3D view of signal-to-noise ratio of each image pixel. *Ellipse* showing minimum SNR peaks corresponds to maximum uncertainty.



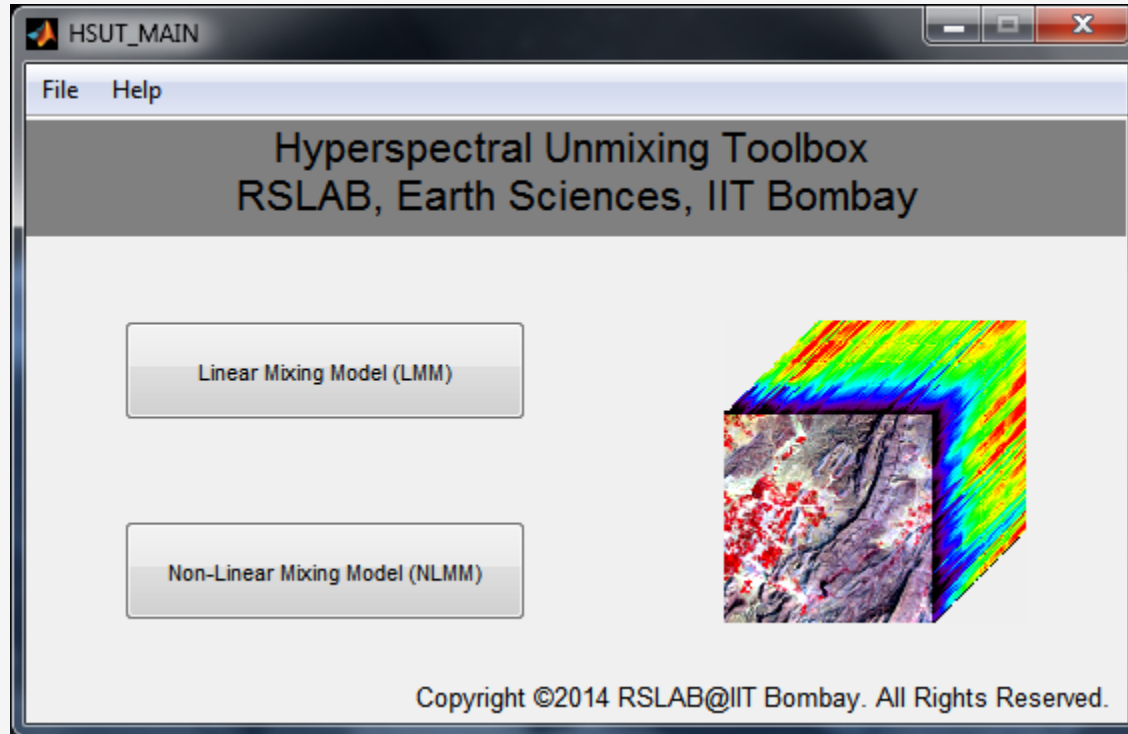
Conclusions:

- The shape and size of the mineral grains (texture), the way they are arranged (pattern) and the source-sensor directions (goniometry) significantly influence the light scattering.
- The experimental data involving bi-, tri- component and multiple boundaries emissivity spectra reveals the effect of texture, fabrics and multi-angular geometry on absorption features (shape and depth).
- These factors can introduce significant errors in geological interpretations whenever conventional LMM is used.
- The mapping uncertainties due to spectral non-linearity in emissive (TIR) domain are caused by coupling of emitted radiances between spatially adjacent heterogeneous samples. Such information is useful for correcting mineralogy of remotely obtained TIR hyperspectral images.

Hyperspectral Unmixing Toolbox (HSUT)

This research has development a software package,

“Hyperspectral Unmixing Toolbox (HSUT), IIT-B”



Web-Link: <https://sites.google.com/site/keshavdevsingh/>



Thank you

Q&A

